SECTION V

QUANTITATIVE DETERMINATION OF ZERO-GRAVITY EFFECTS ON ELECTRONIC MATERIALS PROCESSING — GERMANIUM CRYSTAL GROWTH WITH SIMULTANEOUS INTERFACE DEMARCATION

EXPERIMENT MA-060

By H. C. Gatos,[1,2] A. F. Witt,[1,2]
M. Lichtensteiger,[1] and C. J. Herman[1]

1. Massachusetts Institute of Technology, Cambridge, Massachusetts
2. Co-Principal Investigators

TABLE OF CONTENTS

LIST OF ILLUSTRATIONS

LIST OF ILLUSTRATIONS (Continued)

LIST OF ILLUSTRATIONS (Continued)

LIST OF ILLUSTRATIONS (Concluded)

ABSTRACT

Experiment MA-060 was designed to establish the crystal growth and segregation characteristics of a melt in a directional solidification configuration under near zero-g conditions. The germanium (doped with gallium) system was selected because it has been extensively studied on Earth and because it lends itself to a very detailed macroscopic and microscopic characterization. The interface demarcation technique was incorporated into the experiment since it constitutes a unique tool for recording the morphology of the growth rate throughout solidification, and for establishing an absolute time reference framework for all stages of the solidification process. An extensive study has been performed of the germanium crystals grown during the Apollo-Soyuz Test Project mission. It was found that single crystal growth was achieved and that the interface demarcation functioned successfully. On the basis of the results obtained to date, there is no indication that convection driven by thermal or surface tension gradients was present in the melt. The gallium segregation, in the absence of gravity, was found to be fundamentally different in its initial and its subsequent stages from that of the ground-based tests. None of the existing theoretical models for growth and segregation can account for the observed segregation behavior in the absence of gravity. The results point strikingly to the acute need for extensive experimental and theoretical work on Earth before the far reaching implications of materials processing in space can be understood and exploited.

INTRODUCTION

Gravity-induced convection is always present in the melt undergoing solidification because of the unavoidable thermal gradients. It has also been established that thermal convection causes uncontrollable variations in the rate of crystal growth (or solidification), which in turn result in compositional inhomogeneities and structural defects. Thus, gravity adversely affects the key parameters of the crystal growth (solidification) process. Furthermore, thermal convection interferes with the study of the processing parameters (i.e., rate of solidification, growth interface characteristics, and others) and with the assessment of the relative importance of such parameters in the physical and chemical characteristics of the resulting solids. Since some key materials processing parameters remain essentially unaffected in the absence of gravity, space represents a unique environment and a striking opportunity for materials processing.

Our experiment of indium antimonide crystal growth in the Skylab mission demonstrated beyond doubt that under zero-g virtually ideal conditions of crystal growth can be established, which lead to chemical homogeneity never attained on Earth, and that crystal growth and segregation phenomena can be studied directly in the absence of convective interference.

The present experiment was designed, on the basis of the findings of the Skylab experiment, to obtain more refined fundamental and quantitative information on the crystal growth and segregation processes. The germanium (doped with gallium) system was selected because it has been most extensively studied on Earth for the last 30 years.

OBJECTIVES

The specific objectives of the present Apollo-Soyuz Test Project (ASTP) experiment were to establish the following under near zero-g conditions:

1. The absence or presence of convective phenomena

2. The surface tension (and/or wetting) characteristics of the melt

3. The microscopic growth rate behavior during directional solidification

4. The dopant segregation behavior and its dependence on the microscopic growth rate

5. The heat transfer characteristics of the solidification system.

EXPERIMENTAL APPROACH

To achieve the objectives listed, single crystals grown on Earth were partially melted and resolidified in space with simultaneous transmission of periodic current pulses across the crystal-melt interface.

The growth experiments in flight were carried out in the multipurpose furnace (Fig. V-1) originally designed for the Skylab mission [V-1] and modified to meet higher temperature requirements. The furnace had three tubular cavities into which the stainless steel cartridges containing the crystal assemblies were inserted. Heat levelers, lateral heat shields, and a heat extractor system controlled the heat flow from the heating element through the

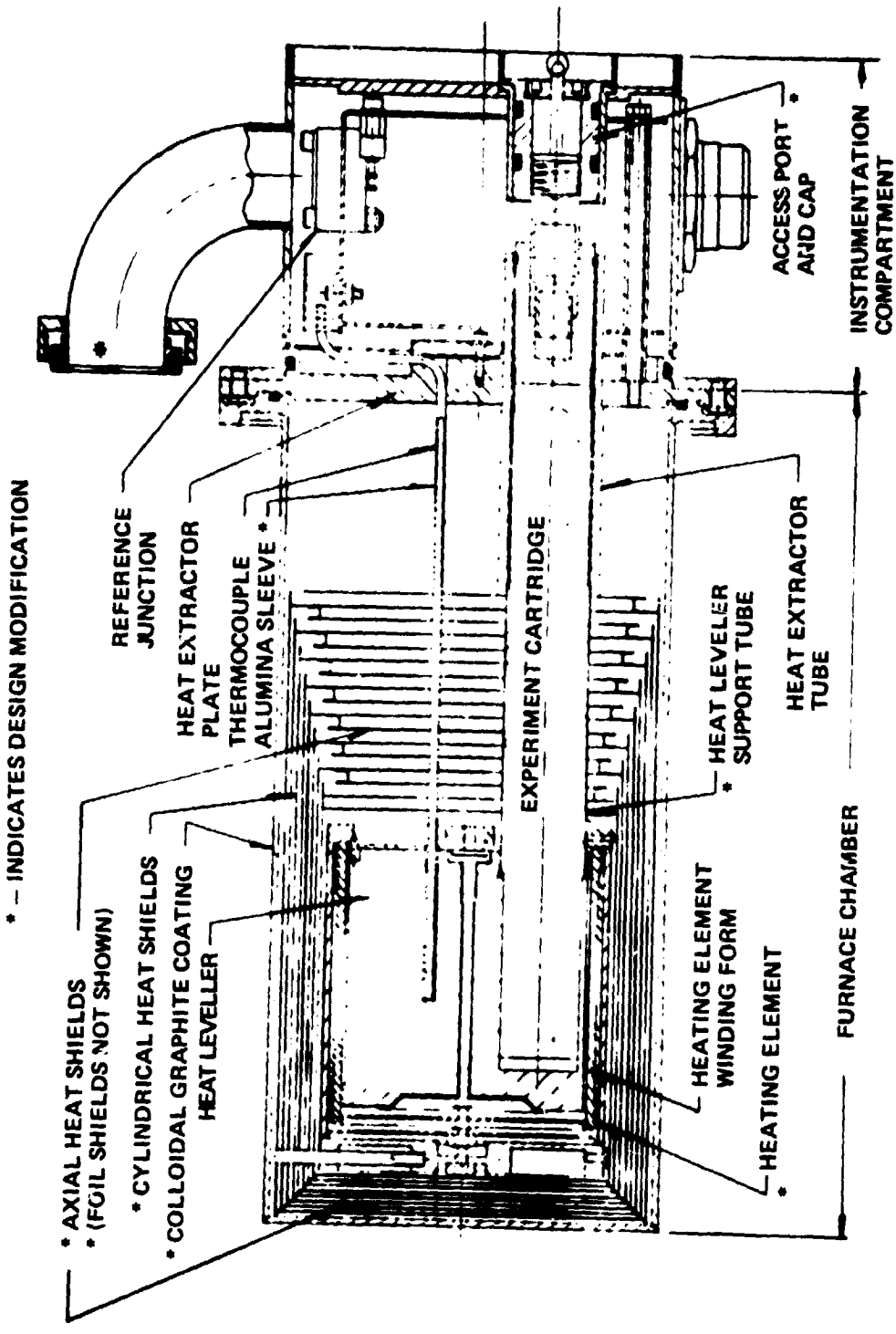

Figure V-1. Schematic of multipurpose furnace designed by Westinghouse for the ASTP crystal growth and solidification experiments.

crystal to the heat extractor plate. In this configuration melting was initiated upon appropriate power input at the crystal end located within the heating element, and the crystal-melt interface was stabilized after 6 cm of each of the original crystals were melted. Stabilization of the crystal-melt interface (thermal soaking) was achieved by reducing the power duty cycle to 90 percent. After thermal soaking (2 h) the power system was switched to the cool-down mode resulting in an average cooling rate of 2.4°C/min. This cooling rate was expected to yield a microscopic growth rate ranging from 5 μm/s at the beginning to 10 μm/s by the end of the controlled cool-down. Controlled cool-down was terminated after 1 h and 23 min (estimated regrowth length of approximately 4 cm); the growth system was subsequently switched to passive cool-down for a period of 1 h and 7 min after which helium was injected into the furnace to accelerate the cooling rate of the system.

To permit growth interface demarcation [V-2] by current pulsing, leads had to be attached to the encapsulated germanium crystals. This was achieved by means of graphite cups at both ends of the crystals to which platinum leads were attached (Fig. V-2). The platinum leads of the three growth systems were connected in series with a power supply that provided current pulses

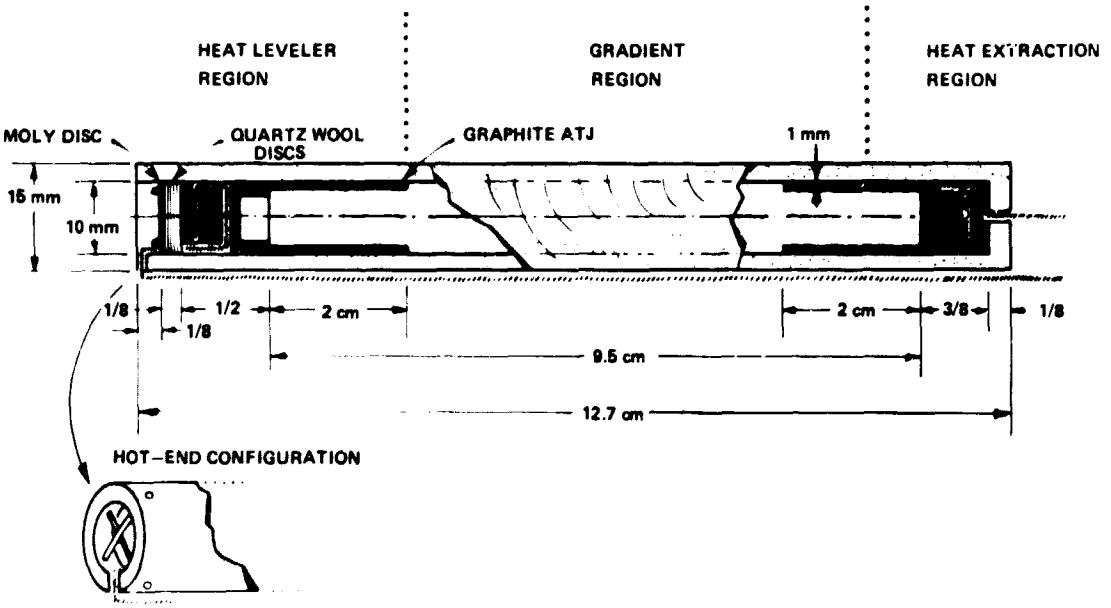

Figure V-2. Ampoule design permitting interface demarcation through current pulsing during regrowth.

(19.1 A/cm^2) of 55 ms duration at intervals of 4 s throughout the experiment, with the seed having a positive polarity. The specific cartridge design and the optimized procedure for interface demarcation were established during extensive ground-based tests, and information concerning this is presented in the appendices.

EXPERIMENTAL RESULTS AND DISCUSSION

The crystals grown in space were subjected to an exhaustive growth and segregation analysis after their return to the Massachusetts Institute of Technology, and this analysis was based on procedures established during ground-based tests. The primary analytical techniques were high resolution etching, Hall effect measurements, spreading resistance measurements, and ion-microprobe analysis. In view of the confined geometry that leads to stresses during growth, no defect analysis of the regrown material was pursued.

Surface Characterization

All crystals regrown in space could readily be removed from their quartz containers (Fig. V-3). In contrast, all crystals grown on Earth could only be isolated by dissolving the quartz containers in hydrogen fluoride (HF). This pronounced difference in behavior of the Earth and space-grown crystals can be understood on the basis of morphological characteristics of their surfaces. In interference contrast it was observed that the crystals grown in space exhibit an irregular network of narrow ridges on their surfaces (Fig. V-4) similar to that observed on indium-antimony (InSb) crystals grown on Skylab. In contrast, all crystals grown during ground-based tests in the same growth facility exhibited surface features that reflect the unavoidable irregularities of the inner walls of the quartz container in detail. It is therefore concluded that no wetting contact existed between the germanium (Ge) melts and the confining quartz ampoules during growth in space, while during growth on Earth the Ge melt is in wetting contact with its confinement. This conclusion is significant since it suggests that effective wetting inversion, first observed during growth of InSb on Skylab, is a phenomenon that may be expected to occur in a multitude of systems subjected to solidification in space. The implications of this effect on materials processing are far reaching with regard to processing technology and possibly with regard to the perfection of materials solidified in partial or total confinement.

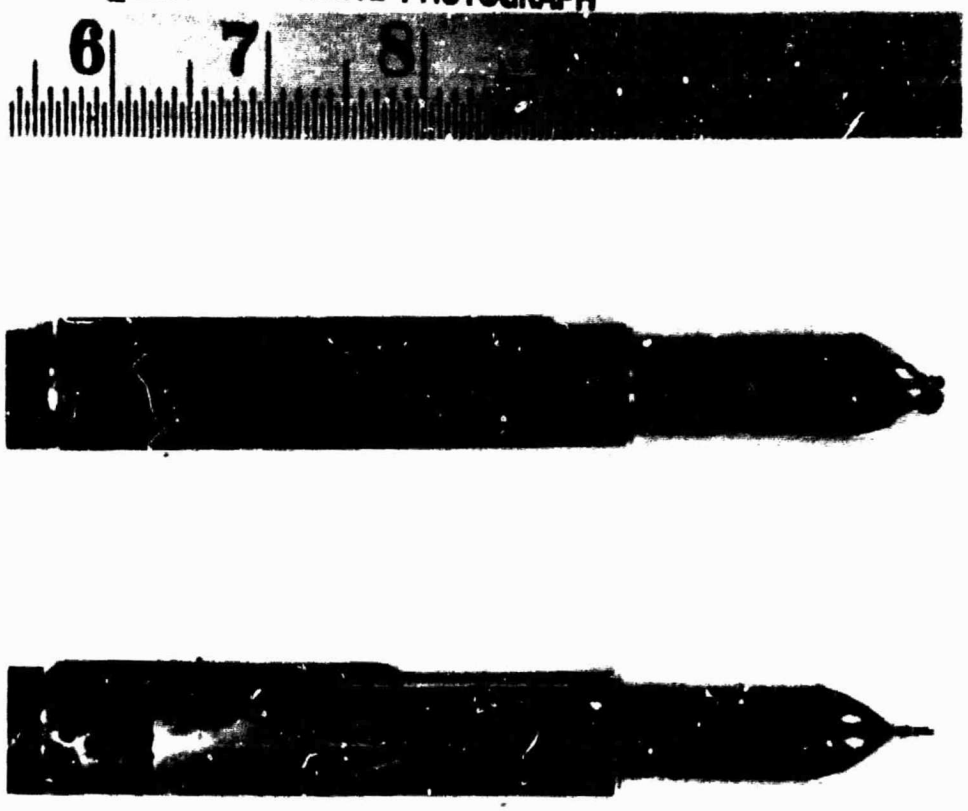

Figure V-3. Germanium crystals of <100> and <111> orientation, regrown in space, after removal from their quartz ampoules.

In all crystals the original regrowth interface was identified (Fig. V-3), which appeared as an abrupt increase (0.5 mm) in crystal diameter at the predicted distance of approximately 3.5 cm from the cold end of the crystals. Its location indicates the extent of back-melting in space and confirms on a macroscale the proper functioning of the multipurpose furnace.

From the morphological characteristics (absence of twin and grain boundaries) it is evident that single crystallinity in the peripheral region of the space grown Ge crystal of <111> orientation prevailed over the entire length of regrowth. In this respect growth in space and growth on Earth are conspicuously different, since all crystals regrown during ground-based tests never exhibited single crystallinity beyond regrowth of approximately 3 cm. The preservation of single crystallinity in the peripheral region (single crystal shell) is particularly remarkable in view of the high doping level for which interface instability due to constitutional supercooling and eventual interface breakdown is

Figure V-4. Irregular ridge patterns on the surface of the <100> germanium crystal regrown in space (180X).

predicted, in fact observed, in the interior of the crystal. Single crystallinity in the peripheral region was not preserved on the space grown <100> crystal. In this case grain boundaries were first observed after growth of 3.5 cm, which compares favorably with ground-based tests where breakdown first occurred after approximately 2 cm of growth.

Bulk Characterization by High Resolution Etching

High resolution etching techniques were refined during ground-based testing to permit the detection of microscopic compositional fluctuations in Ge with a sensitivity of better than ±0.2 percent at gallium-dopant levels in excess of 10^{18} per centimeter. Bulk characterization by etching was performed on longitudinal center cuts of the regrown segments. The exposed surfaces were polished and etched (see the appendices). Figure V-5 shows an etched segment of the <111> Ge crystal regrown in space. Three regions can be identified: the original seed portion (top), a narrow region exhibiting microscopic compositional inhomogeneities, and a region exhibiting no compositional fluctuations (bottom). The latter growth region exhibits faint, but distinct, lines that are the current-induced interface demarcations formed at intervals of 4 s during regrowth. It can be seen that the spacing of consecutive demarcation lines converges to zero (zero growth rate) at the lower end of the bandlike region of perturbed growth and segregation. Thus, interface demarcation establishes that the formation of the growth region with compositional fluctuations (band below the original regrowth interface) took place during the 2 h thermal soak and preceded the controlled regrowth. Ground-based tests indicated that this growth band reflects thermal instability of the furnace and is attributed to a slight imbalance of heat input and heat loss during the early stages of thermal soak (see the appendices).

Etching analysis revealed further that the bulk of the controlled regrowth region of the <100> crystal is free of microscopic compositional fluctuations over a grown length in excess of 2.5 cm. For regrowth in the <111> direction minor compositional fluctuations of approximately 0.1 percent were observed associated with peripheral facet formation (Fig. V-6); the nature of there perturbations is not as yet understood.

Segregation inhomogeneities associated with interface breakdown due to constitutional supercooling were observed in all crystals after the advancing growth front had moved into the graphite cup. The breakdown in the space grown material is attributed to deteriorating thermal gradients caused by abrupt changes in the thermal conductivity of the confinement system (in going from

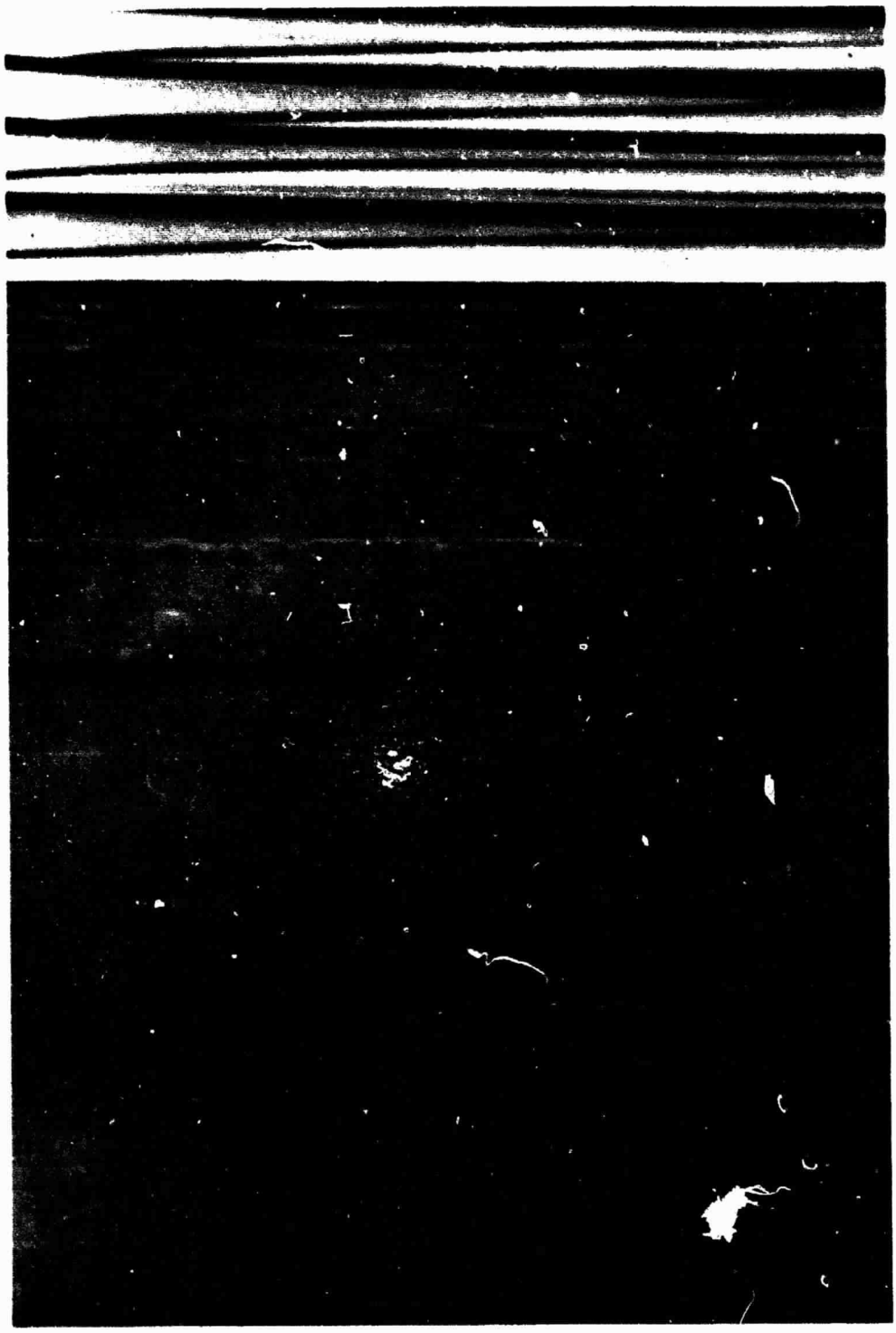

Figure V-5. Etched segment of the [111] germanium crystal regrown in space; observe the seed portion (top) and the controlled regrowth portion (bottom) separated by a band of uncontrolled growth and segregation (140X).

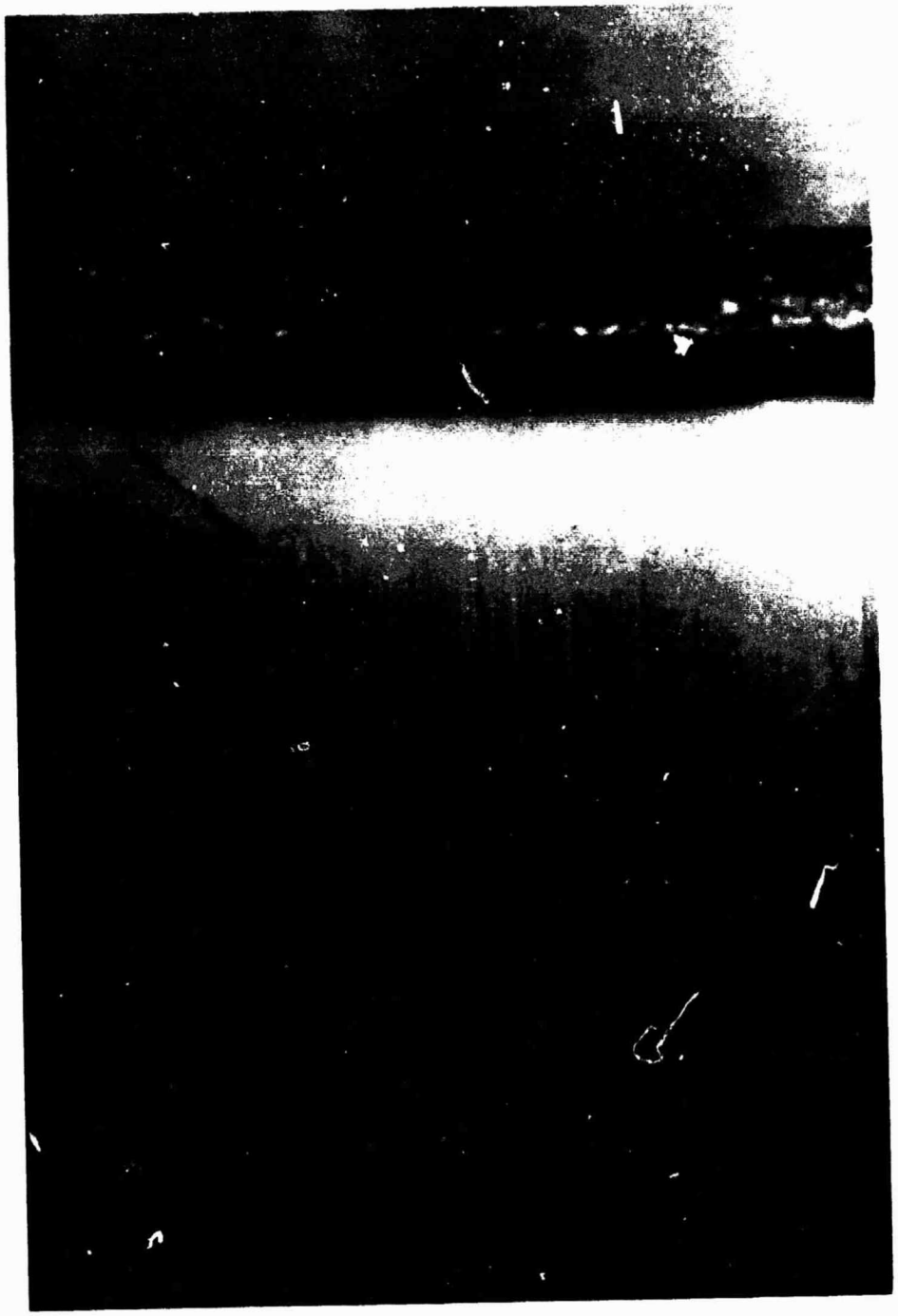

Figure V-6. Segregation inhomogeneities associated with peripheral facet formation in the <111> germanium crystal regrown in space (375X).

quartz to graphite) and the resulting changes in the growth interface morphology. It is important to note that the onset of instability occurs significantly earlier in the <111> crystal and is initiated at the facet to off-facet boundary. On occasions, the morphological characteristics of the unstable growth interface are much more regular and conforming to theoretical predictions in the space-grown crystals than in those grown on Earth (Figs. V-7 and V-8).

Growth Behavior on the Microscale

From interface demarcation lines introduced at intervals of 4 s, a quantitative growth rate analysis on a microscale was obtained for all space-grown crystals. The rate data for the crystals grown in the <111> direction are shown in Figure V-9. It can be seen that during the early stages of the cooling cycle, the microscopic rate of growth increases rapidly from zero to approximately 7 μm/s. After the initial transient region, the rate increase slows down and after approximately 2.5 cm of growth, the microscopic growth rate approaches a value of 10.5 μm/s. The growth rate behavior observed in space (for the cooling rate of 2.4°C/min) is virtually identical with that encountered during ground-based testing and indicates that the heat transfer characteristics of the system are the same in space and on Earth. This result indicates that in the growth configuration used, conductive heat transfer dominates and the contribution of laminar convection to heat transport, which is present in the ground-based tests, is negligible.

It should be pointed out that all existing theories of segregation assume an initial step function of the growth rate from zero to a finite and constant rate; since all real melt growth systems exhibit an initial transient growth behavior, no quantitative comparison between theory and experiment can be made. In view of these results, the development of a modified segregation theory has been initiated that considers the existence of initial growth rate transients under convection-free conditions.

Dopant Segregation Behavior

Quantitative compositional analyses of crystals regrown in space and on Earth have been obtained through spreading resistance measurements with a linear resolution of 5 μm. The results obtained for the initial regrowth region of crystals grown in the <111> direction are shown in Figure V-10. (These regions are the same as those shown in Figure V-5.) The measurements taken along the growth direction of a ground- and flight-grown sample identify three

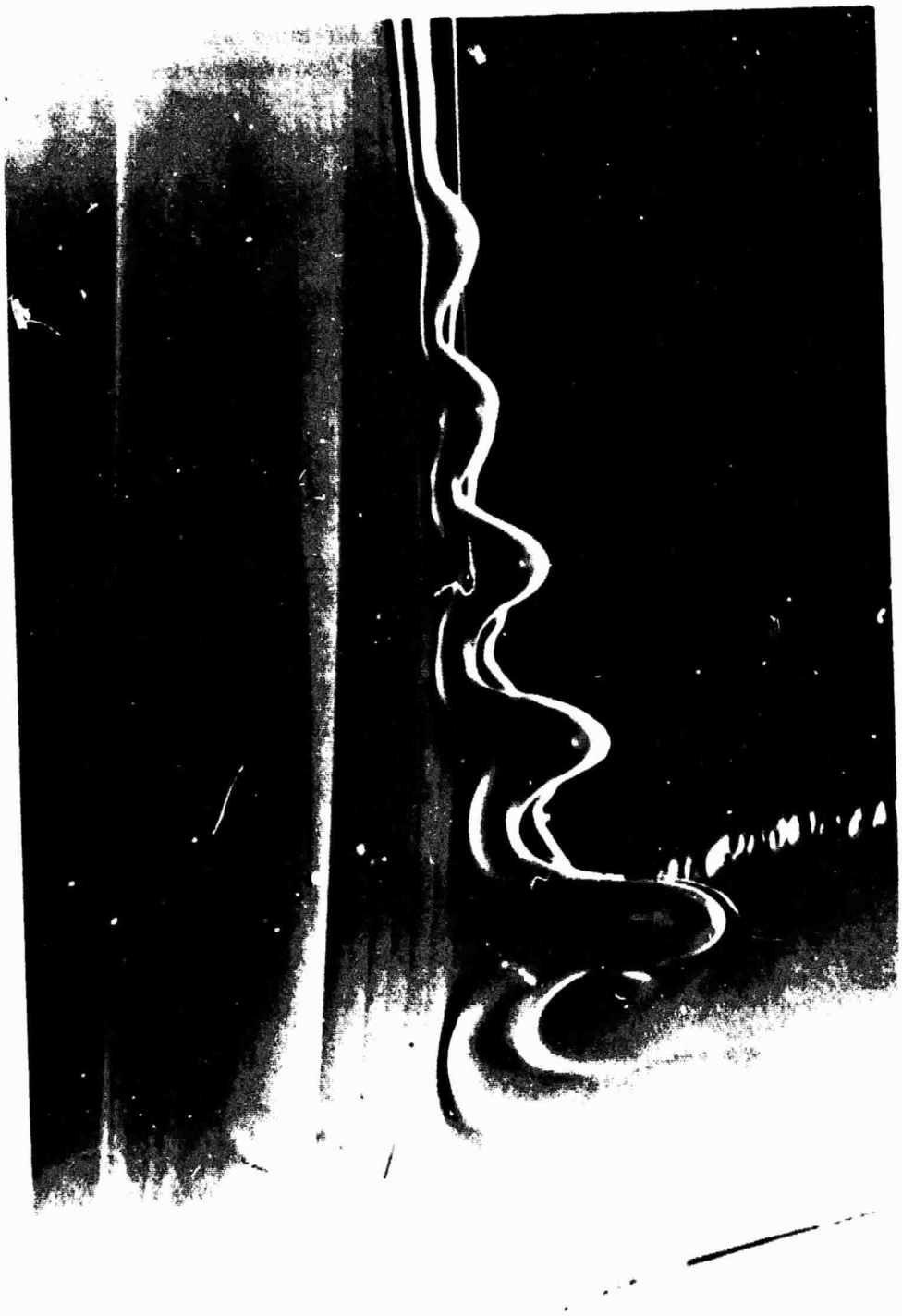

Figure V-7. Frontal interface breakdown during late stages of <111> germanium regrowth in space (compare with Figure V-8) (300X).

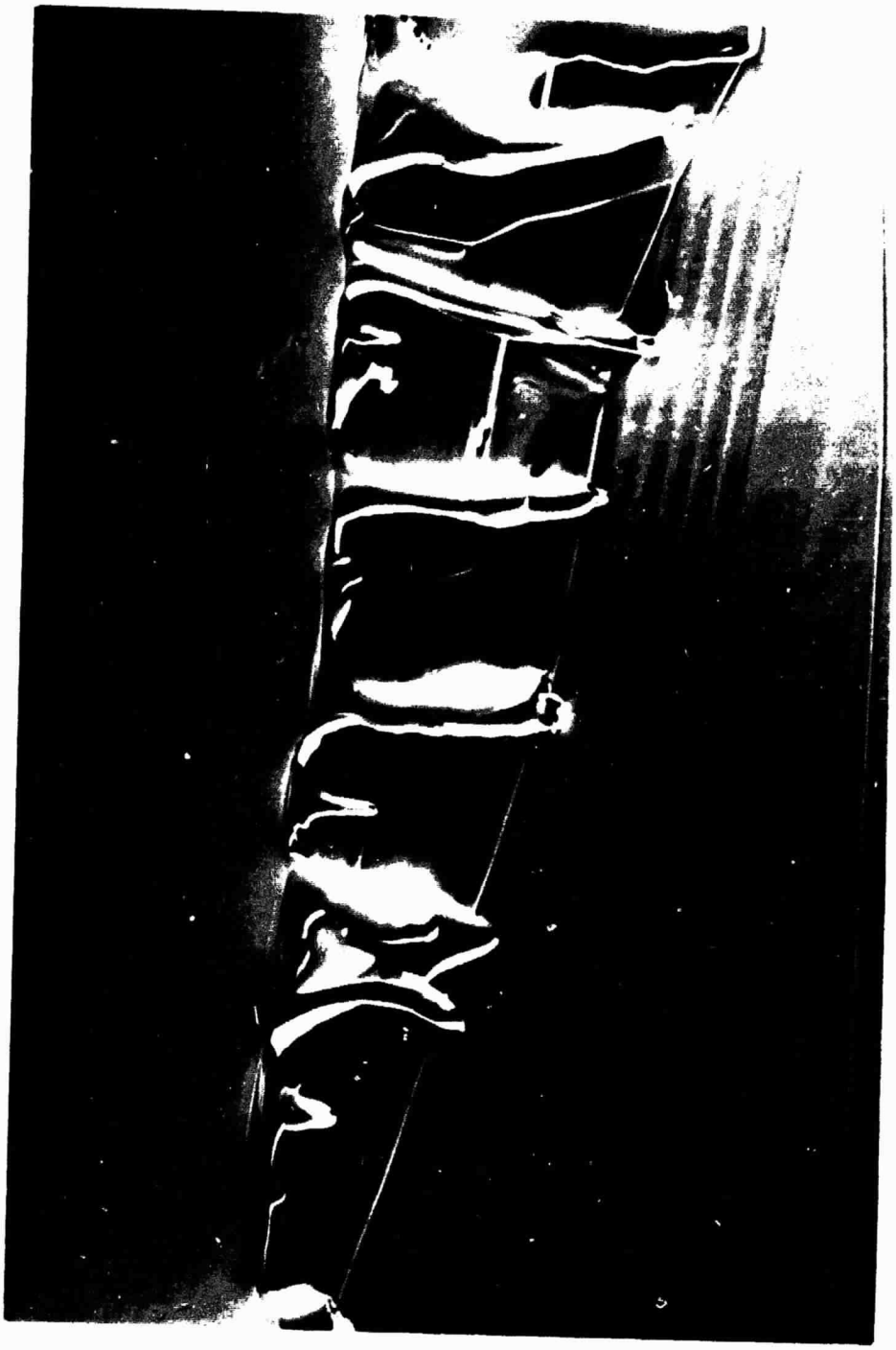

Figure V-8. Frontal interface breakdown during late stages of <111> germanium regrowth on Earth (300X).

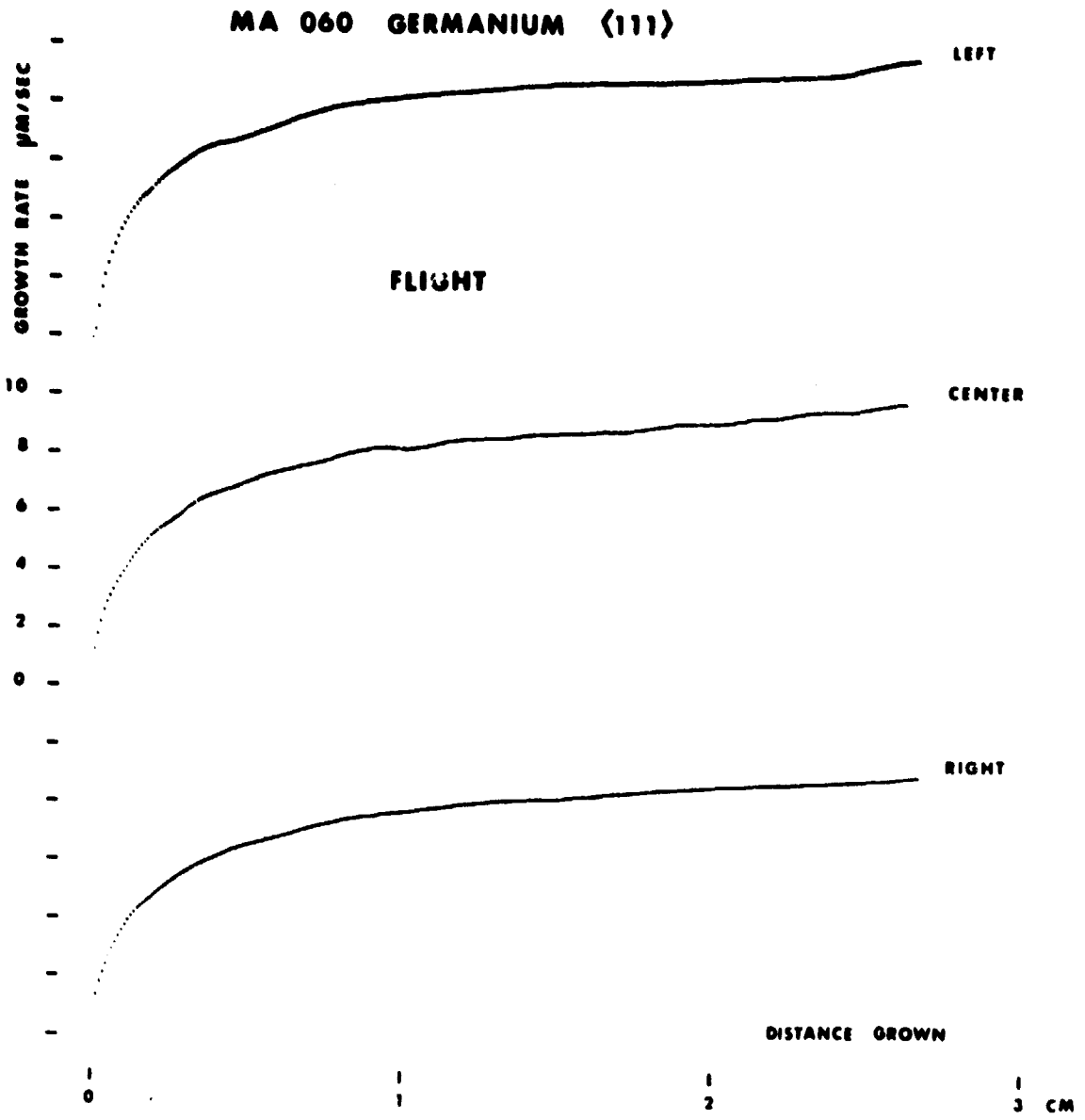

Figure V-9. Microscopic growth rates of the <111> germanium crystal regrown in space.

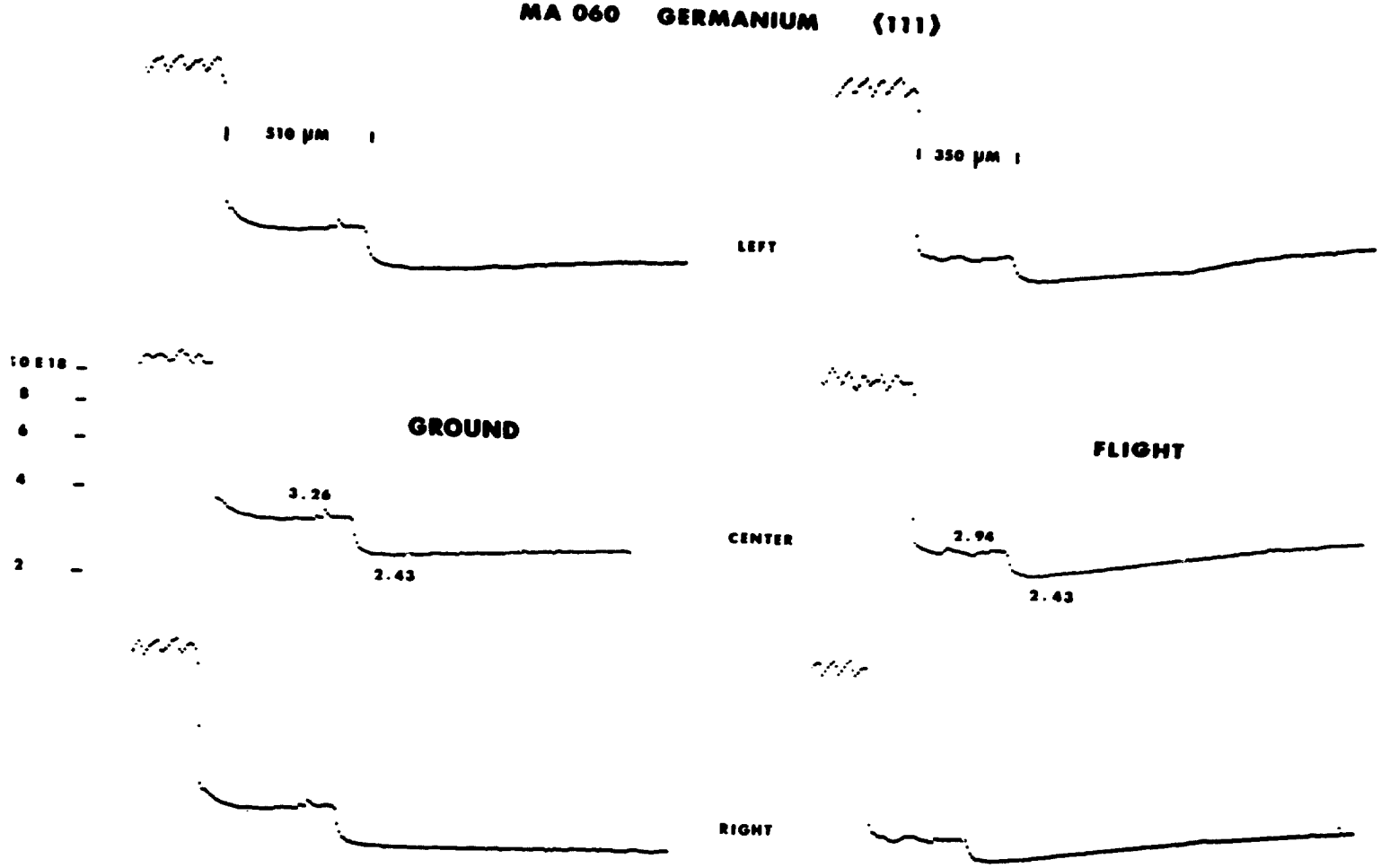

Figure V-10. Compositional profiles of the initial regrowth region in the <111> germanium crystal regrown in space; ground-based data shown for comparison.

regions: the seed regions on the left, characterized by pronounced compositional fluctuations; the bands of uncontrolled growth in the center; and the regrown regions with steadily increasing dopant concentration on the right. It is seen that the initial region in the space grown crystal exhibits a much more rapid dopant concentration increase than the crystal grown on Earth. This behavior reflects the effect of laminar convection on segregation. The results are not, however, as expected with regard to the absolute dopant concentration level. Taking the equilibrium distribution coefficient (k_o) of gallium (Ga) in Ge to be 0.087, as generally accepted, the dopant concentration in the initial regrowth region should assume a value of approximately 9×10^{17} per cubic centimeter instead of the presently measured value of 2.43×10^{18} per cubic centimeter. Since virtually identical initial dopant concentration levels were observed in both samples, it is assumed that the generally accepted value for k_o is erroneous.

The appearance of growth facets in the space-grown <111> crystal made it possible to study the facet segregation behavior in the absence of convective interference. The spreading resistance measurements (Fig. V-11) show that the dopant concentration on-facet is less than that of off-facet by a factor of 0.92. The tracings further show that the compositional change on-facet to off-facet takes place over a distance of approximately 30 μm.

Attempts to analyze quantitatively the initial segregation transient in the regrowth region of the space grown sample failed because of the existing growth rate transient, which is not considered in the theoretical treatments. In view of the unavailability of reliable values for k_o and D, the diffusion coefficient essential for a quantitative segregation analysis, appropriate experiments under zero-g conditions must be performed for the accurate determination of these constants.

Compositional analysis on a macroscale, covering the whole length of crystals regrown in space, is still being pursued. The results obtained to date are to a large extent unexpected and as yet unexplained. As seen in Figure V-12 the dopant concentration, as expected, increases steadily over a distance of approximately 1.5 cm from the original regrowth interface. At this distance k_{eff} approaches the value of 1, characteristic of diffusion-controlled steady-state segregation. However, with continuing growth and with a steadily increasing microscopic growth rate, the dopant concentration decreases instead of reaching the steady-state value. The dopant concentration continues to decrease over a distance of approximately 1 cm of growth. At this point interface breakdown takes place, due to constitutional supercooling, and a further analysis of the segregation behavior is not possible.

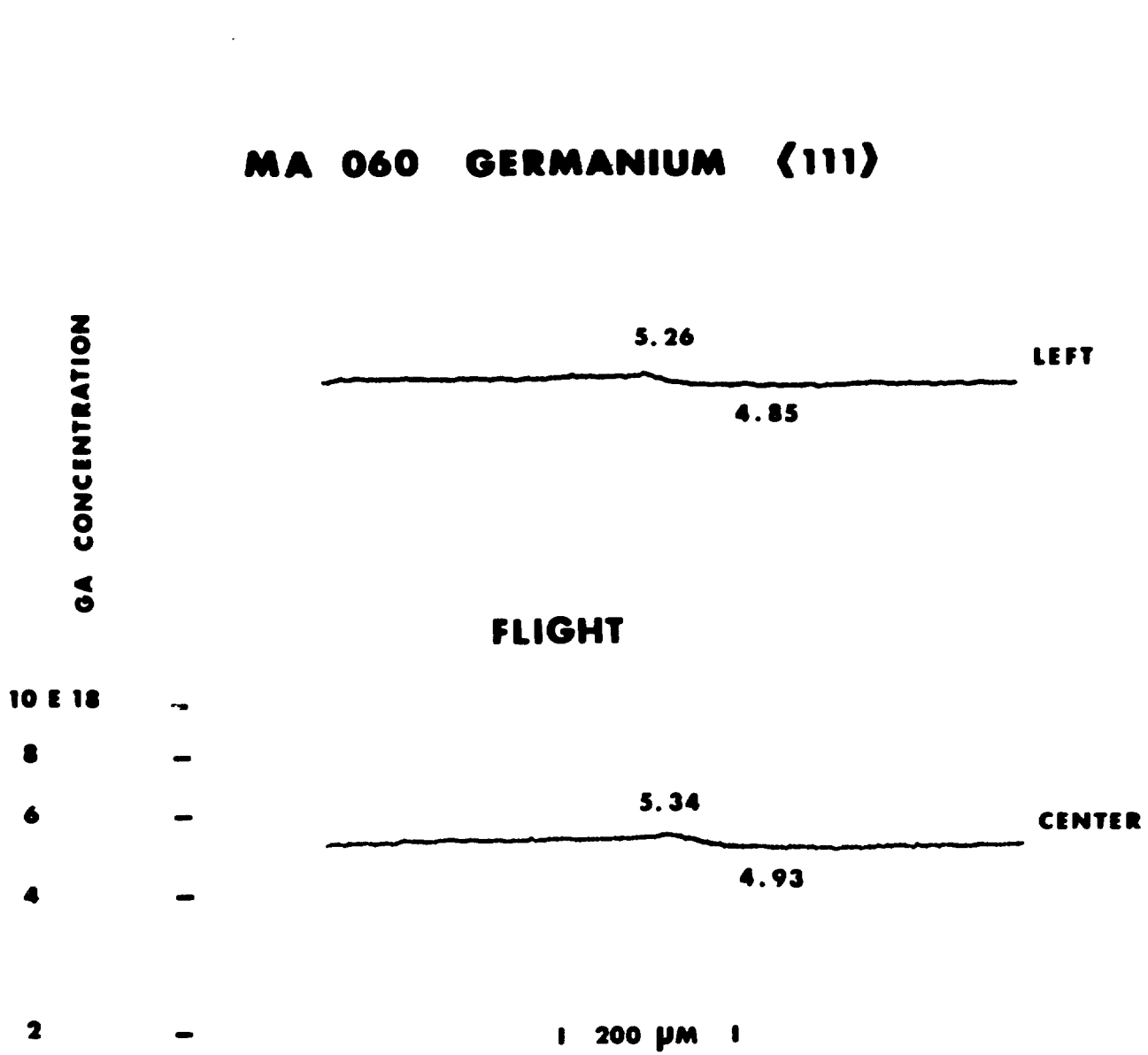

Figure V-11. Compositional profile of the off-facet to facet transition region in the <111> germanium crystal regrown in space.

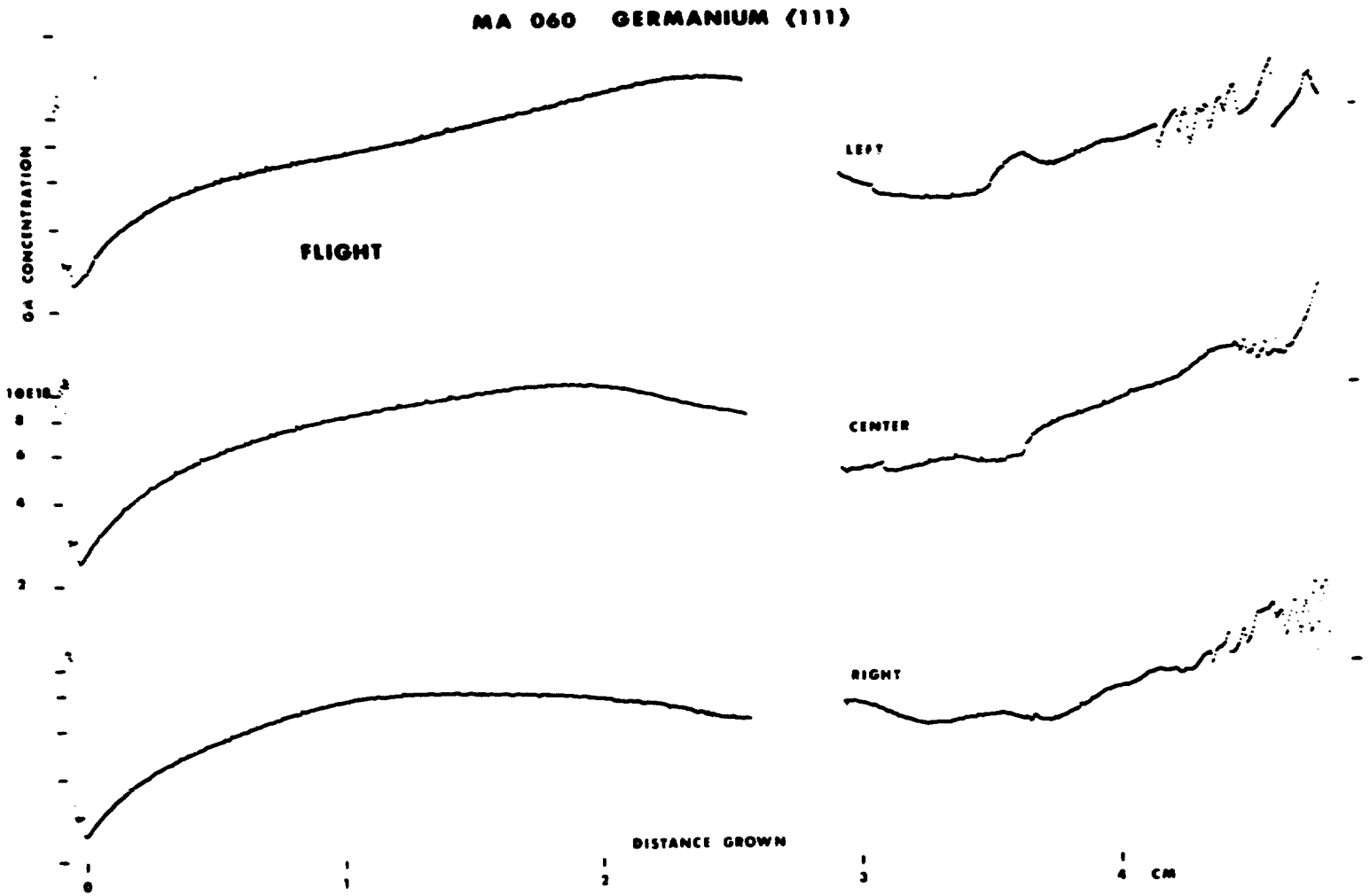

Figure V-12. Macroscopic compositional profile of the <111> germanium crystal regrown in space.

There are indications that the observed segregation anomaly is not characteristic of growth under zero-g conditions, but that it is a consequence of the particular geometry of the growth system.

In view of the potentially far reaching implications of these unexpected segregation effects, a complete understanding of their origin is of paramount importance.

SUMMARY

The present experiment revealed growth and segregation effects previously not observed on Earth. The bulk of these effects cannot be accounted for by an existing experimental or theoretical models of growth and segregation. This finding has fundamental implications in view of the fact that germanium is the most studied and best understood among all solids. It clearly implies that, although the uniqueness of outer space for materials processing is a truism, exploitation of the unprecedented opportunities of the zero-g environment necessitates the selection of systems and experimental apparatus that have been or can be exhaustively investigated on Earth, so that the effects of zero-g conditions on materials processing can be unambiguously indentified and quantitatively studied. It further implies that extensive research is essential following space experimentation, even on critically selected and well understood systems, to quantitatively understand the zero-g effects and establish sound guidelines for subsequent space processing. It is the belief of these investigators that materials processing within the Shuttle program, without major expansion of ground-based investigations on critically selected materials systems, is likely to evolve into a most expensive and unprofitable undertaking.

APPENDIX A

GROWTH OF GERMANIUM CRYSTALS FOR GROUND-BASED TESTS AND FLIGHT EXPERIMENTS

All germanium single crystals (23) used for the experiments were pulled from doped melts by the Czochralski technique under the following growth conditions:

Ge Charge:	240 g in ATJ graphite crucibles
Dopant Elements:	Ga, tin (Sn), and antimony (Sb) (all crystals were singly doped)
Doping Levels:	The melts were doped to achieve an average dopant concentration of approximately 10^{18} to 10^{19} per cubic centimeter in the grown crystals.
Seed Orientation:	<100> and <111>
Protective Gas Atmosphere:	H_2 at a pressure of approximately 760 760 mm Hg
Pulling Rate:	2 in./h for Ga doped crystals 1 in./h for Sb and Sn doped crystals
Seed Rotation:	10 rpm
Crucible Rotation:	0 rpm

The crystals (weight of approximately 130 g, length of approximately 15 cm, and diameter of approximately 1.5 cm) were centerless ground to a diameter of 1.046 cm and cut to a length of 9.5 cm. The diameter of both ends of all crystals was reduced to 0 843 cm over a length of 2.06 cm to permit the attachment of graphite cups which served as the current contacts for interface demarcation. The crystals were subsequently etched in CP-4 (five parts HNO_3, three parts HF, and three parts CH COOH, Br_2) to the desired diameter of 0.838 cm. Samples from both ends of all crystals were retained for the determination of the doping levels.

APPENDIX B

AMPOULE DESIGN AND ASSEMBLY

The ampoules confining the growth systems were made from heavy wall quartz (Amersil) tubing (inside diameter of 10 mm, outside diameter of 16 mm) which was centerless ground to 1.50 cm diameter and cut to a length of 12.7 cm. Prior to assembly the ampoules were etched with HF; rinsed with distilled H_2O, methanol, and acetone; and dried with hot filtered air. The graphite contact cups, machined to yield low contact resistance with the germanium crystals, were fired at 1600°C in a vacuum of 10^{-7} torr; subsequently platinum leads were attached as shown in Figure V-1.

After a discussion with the technical staff of Westinghouse, it was decided to use an open ampoule configuration (non-vacuum tight) with 0.04 in. Pt current leads and graphite cups at both ends of the crystals as contacting media (Fig. V-2). The inside length of the graphite cups was 2.0 cm and designed to ensure contact with the melt irrespective of the degree of back-melting. The mechanical contact design required precision machining of the graphite cups and the germanium crystals. The ampoule design was tested in ground-based experiments and was used for the flight experiment without modification.

APPENDIX C

PULSE POWER SUPPLY

From preliminary experiments it was concluded that growth characterization on a microscale through interface demarcation would require a power supply capable of delivering current pulses of the following characteristics (Fig. V-13):

Pulse Repetition Rate:	2 s
Pulse Duration:	$\geq$ 75 ms
Amplitude:	25 A independent of load resistance variations up to 1 Ω

The basic design criteria of the pulse power supply and its connection to the three growth ampoules in either parallel, series, or a multiplexed (sequential) configuration were evaluated jointly by members of the technical staff of Westinghouse and Massachusetts Institute of Technology.

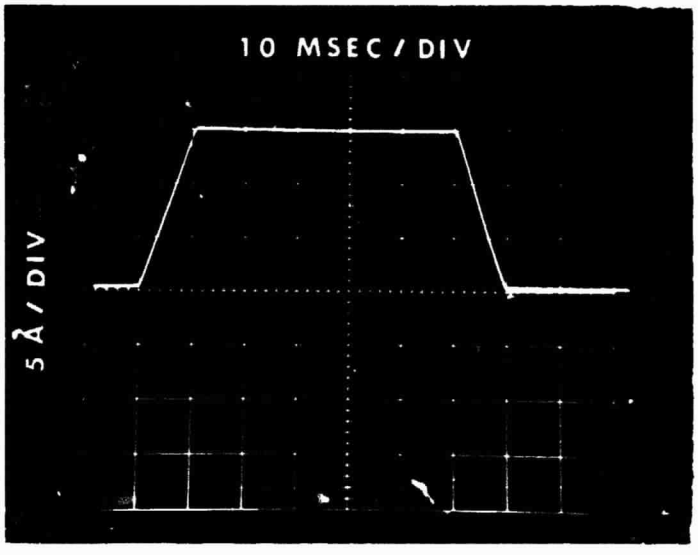

Figure V-13. Characteristics of pulses used for interface demarcation during flight experiment.

On the basis of the power available for MA-060, a prototype unit to be connected in series with the growth ampoules was designed that delivered 50 ms half-width constant current pulses of 15 A amplitude into a resistive load of up to 1 Ω with a nominal repetition rate of 4 s. The pulse transit time was degraded to 10 ms to minimize electrical isolation requirements for the spacecraft power bus.

APPENDIX D

SAMPLE PREPARATION FOR ETCHING ANALYSIS AND SPREADING RESISTANCE MEASUREMENTS

For bulk crystal analysis by interference contrast microscopy and spreading resistance measurements, all crystals were cut along the growth direction to obtain 0.2 cm thick slices containing the crystal axis. These center cuts were mounted on brass disks, as described in the following, and their surfaces were ground with 10 μm abrasive. All samples were subsequently mechanically polished to a Linde A surface finish and chemically polished with a modified Syton HT 30 solution (200 ml Syton HT 30, 200 ml H_2O, 5 ml H_2O_2, and 2 ml CH_3COOH). The samples were then etched by immersing them for 5 to 8 s in a solution of one part HF, one part CH_3COOH, and one part H_2O. For quantitative segregation analysis, the specimens were first subjected to spreading resistance measurements and subsequently investigated by interference contrast microscopy. With this procedure it was possible to determine the microscopic growth rate (from the spacing of consecutive interface demarcation lines) corresponding precisely to the region for which the dopant concentration profile was obtained through the spreading resistance measurements (the traces of the spreading resistance probe are visible in interference contrast). Photomicrographs were taken with Contrast Ortho Film (125 ASA).

APPENDIX E

SPREADING RESISTANCE MEASUREMENTS

The functional relationship between resistivity ρ and spreading resistance R_s with its application to the "spreading resistance probe" technique has been described by Mazur [V-3]. Resistivity and mobility data for germanium at 300°C have been analyzed by least-square methods and plotted as a function of impurity concentration by Sze and Irvin [V-4], which then establishes an exact correlation between spreading resistance and impurity concentration. Thus, spreading resistance measurements provide an elegant way of determining dopant impurity profiles on a microscale [V-5].

All measurements were performed with a single probe, which was calibrated against a small segment of the germanium <111> flight crystal, 0.4 cm × 0.4 cm × 0.2 cm in size, as a standard. Its resistivity and carrier concentration were determined by Hall effect measurements at 300°C using the Van der Pauw technique [V-6].

Center slices of 0.2 cm thickness were diamond-wheel cut from the ASTP flight and their corresponding ground-based test crystals. Due to the 2.5 cm traverse limit of the X-axis drive of the probe positioner, each slice had to be cut, which prevented continuous scanning of the sample surfaces.

Large area ohmic contact to the back side of all samples to be analyzed was made with an evaporated and microalloyed silver layer. The samples were pressure-bonded to brass disks with conductive silver paint.

Subsequently, the samples were polished and etched as described previously.

Reproducibility of the measurements taken on stabilized surfaces was better than 2 percent for the <111> germanium segments and approximately 5 percent for the <100> germanium segments (worst case). Occasional excessive data scatter on systematic drift of the data base could in all cases be traced to steps in the sample preparation.

The raw spreading resistance data were first converted to normalized resistances using a quadratic regression fit, correcting for additional distributed resistances in the external circuitry. From these values, resistivities were calculated without smoothing and fitted to a computer-generated expression for the concentration versus resistivity relationship employing a spline cubic interpolating polynomial. The resulting concentration values were plotted as a function of distance on a high speed digital plotter.

APPENDIX F

GROUND-BASED TESTS

Simulation Tests

The purposes of simulation tests were: (1) to study the thermal characteristics of the ampoule design, (2) to determine the cartridge design that would yield specified growth characteristics in the multipurpose furnace, and (3) to test growth interface demarcation.

The simulation tests indicated that the growth procedure used by Westinghouse resulted in Ge regrowth of 2.2 cm instead of the specified value of 3.0 cm. It was also observed that the intensity of interface demarcation (for pulses of 30 ms duration) over the first 1.5 cm of regrowth is too low to be detected by etching. Since growth experiments in the laboratory with the same pulse characteristics yielded detectable interface demarcation, it was concluded that current leakage in the simulation test arrangement was responsible for the lack of adequate interface demarcation.

To ensure detectable growth interface demarcation it was subsequently requested that the pulsing frequency be changed from 0.5 to 0.25 Hz and that the duration of the current pulses be increased from 30 to 60 ms.

Prototype Tests

These tests served to finalize ampoule and cartridge design as well as the pulse characteristics for interface demarcation; in addition, these tests were used to evaluate the detectability of interface demarcation in Sb and Sn doped germanium crystals. It was found that current pulses of 15 A and 60 ms duration lead to detectable interface demarcation in Ga doped crystals but not in Sb and Sn doped crystals. On the basis of these experiments, it was furthermore concluded that the desired regrowth rate (approximately 5 μm/s) could best be approximated at a cooling rate of 2.4°C/min.

Ground-Based Tests (GBT)

A total of three ground-based tests, each involving a melting and regrowth of three crystals in the prototype furnace, were carried out at MSFC. During these tests the cool-down rates, pulse characteristics, and pulse polarity was

tested. It was observed that furnace stability and the resulting regrowth characteristics were significantly affected by the lack of stable line voltage. In subsequent GBT experiments the furnace was battery operated and the pulse characteristics optimized at seed polarity (+), 0.25 Hz, 15 A, and 6 ms duration. The experiments further confirmed that a cooling rate of 2.4°C/min approximates the specified regrowth rate on Earth. The last GBT experiment, during which all specified growth and interface demarcation characteristics were applied, was performed in the prototype furnace after the actual launch of the ASTP mission. The results obtained during this test were used as reference for the space grown crystals.

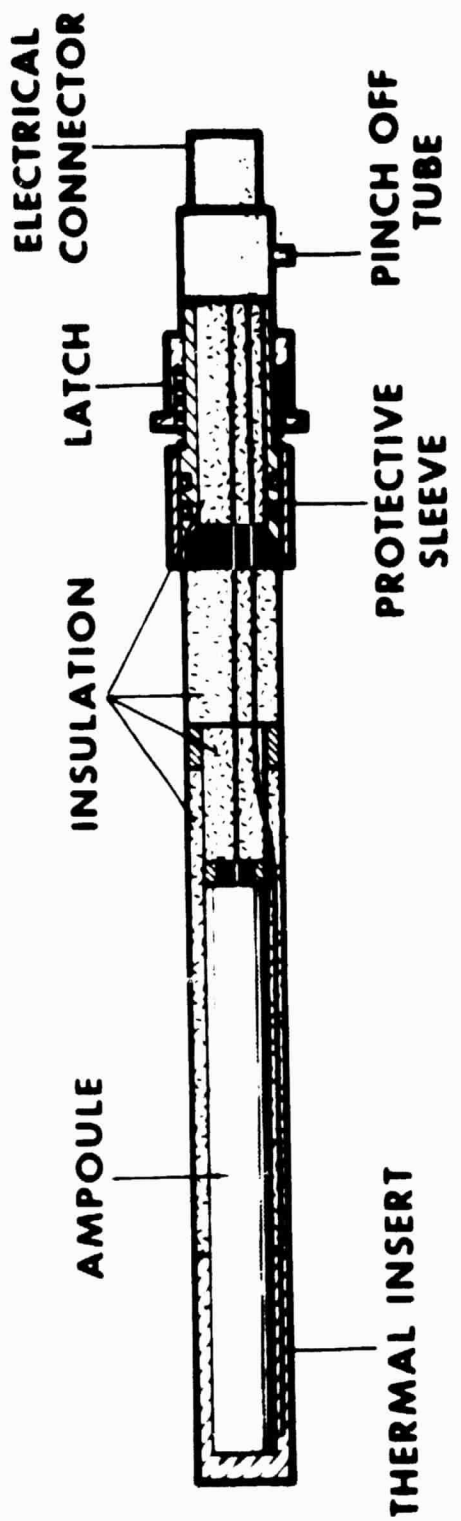

Figure V-14. Schematic of cartridge design for experiment MA-060.

Figure V-15. Cartridges used for ground-based and flight experiments.

ORIGINAL PAGE
BLACK AND WHITE PHOTOGRAPH

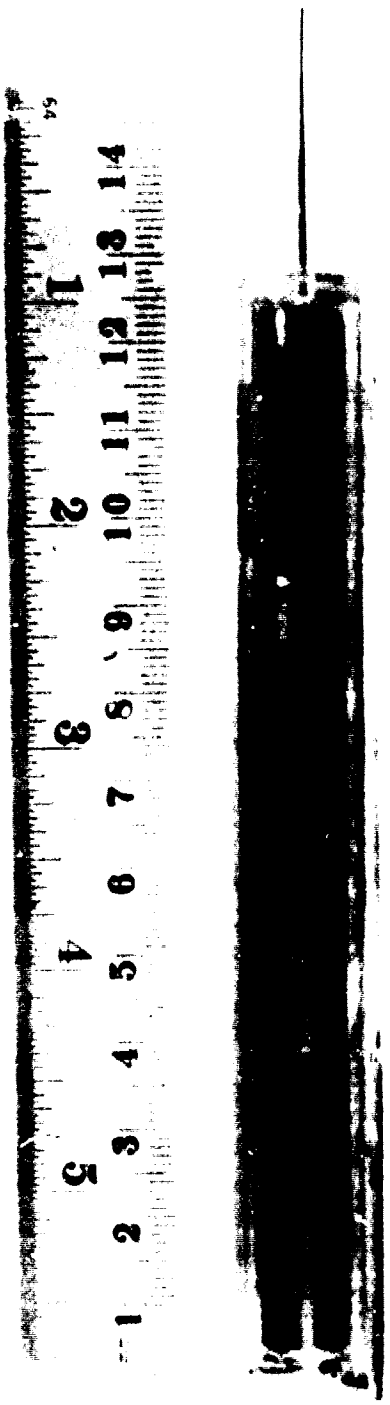

Figure V-16. Encapsulated germanium crystal used for simulation tests (the ampoule in the configuration shown was used for all ground-based and flight experiments).

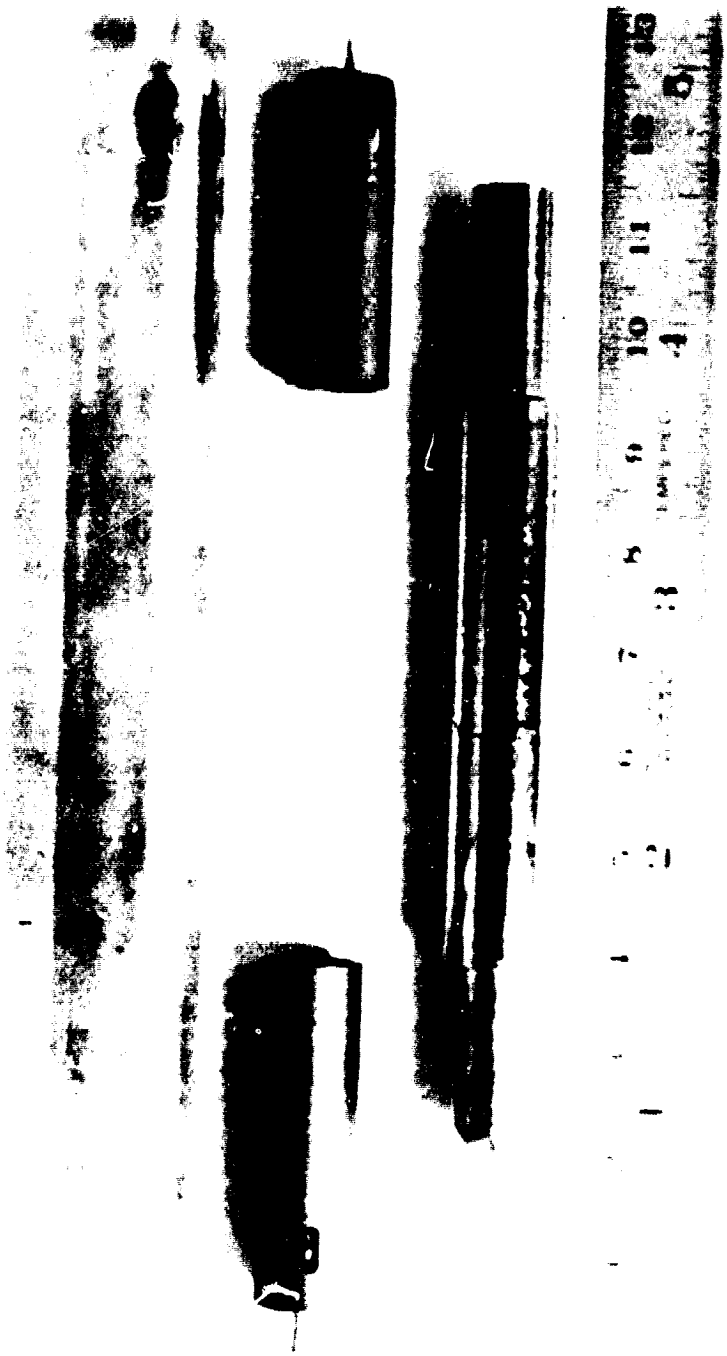

Figure V-17. Isolated germanium crystal regrown during simulation test (length of regrowth was 2.2 cm; the graphite cups which serve as contact material for current pulsing are also shown).

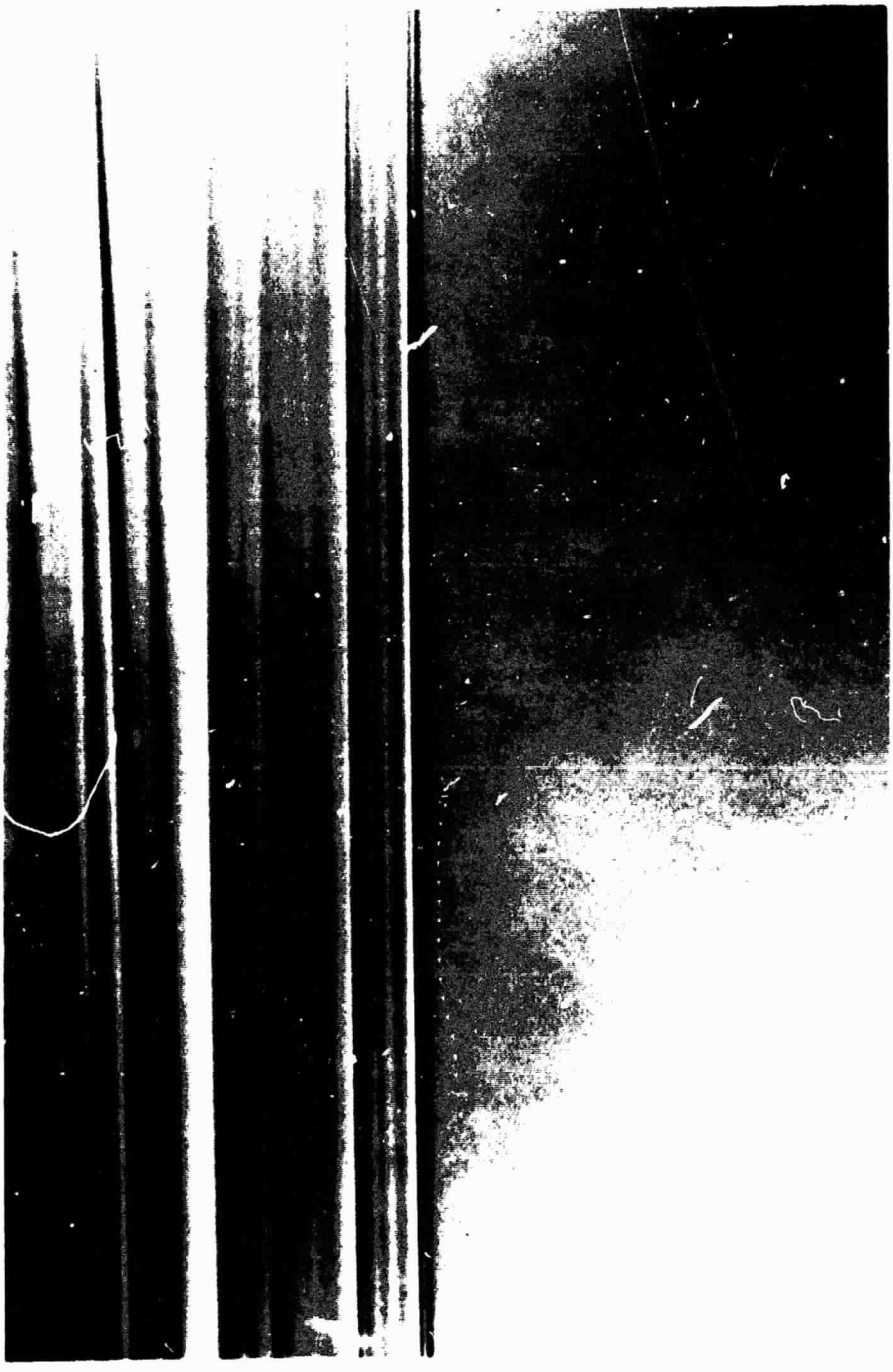

Figure V-18. Etched segment of germanium regrown during simulation test (notice the band of uncontrolled growth (200 μm) formed prior to passive cool-down; notice further that interface demarcation is not revealed by etching) (140X).

Figure V-19. Etched segment of the germanium crystal regrown during the prototype test (notice the absence of uncontrolled growth prior to controlled cool-down; the growth conditions involved a slight temperature increase prior to initiating the cool-down cycle) (140X).

Figure V-20. Interface demarcation achieved by current pulses of 15 A and 60 ms duration at a repetition rate of 4 s (the crystal shown was pulled, by the Czochralski technique, during ground-based testing).

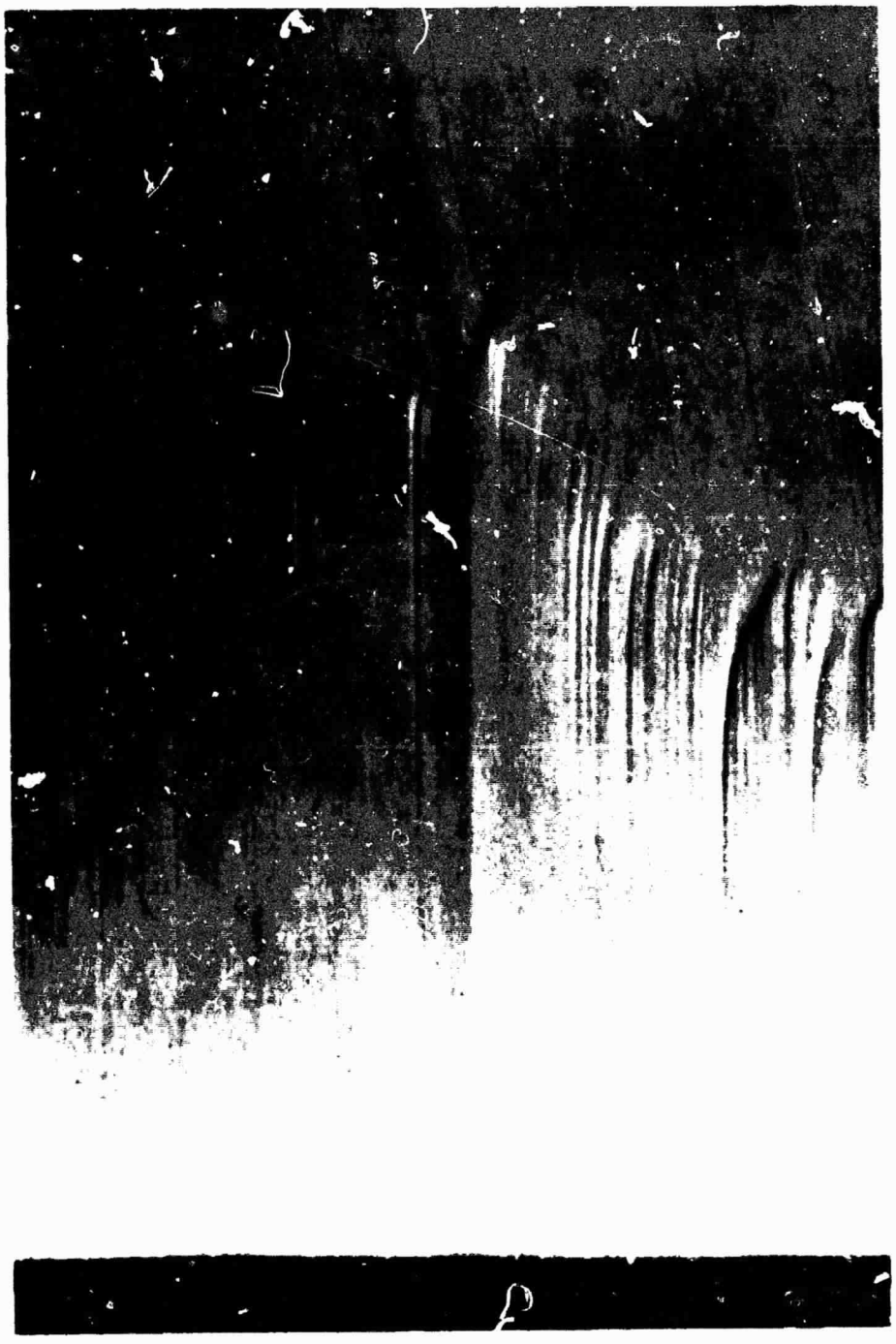

Figure V-21. Etched segment of a <111> germanium crystal regrown under conditions simulating the multipurpose furnace configuration (notice the pronounced interface demarcation achieved by current pulses with characteristics similar to those provided by the Teledyne-Brown pulsing unit).

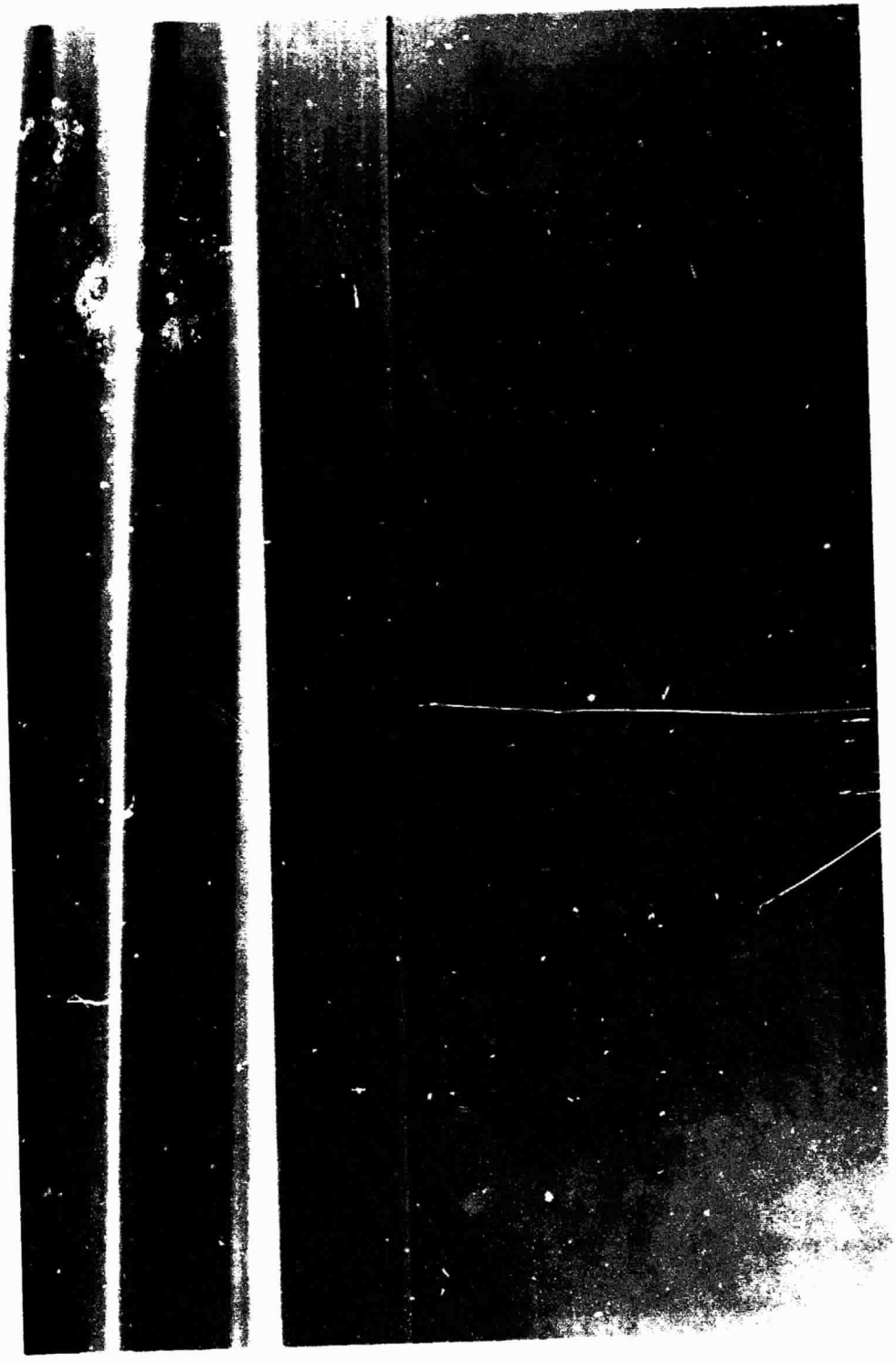

Figure V-22. Etched segment of <111> germanium crystal regrown during ground-based testing (notice the well delineated interface demarcation achieved by current pulses of 15 A and a duration of 50 ms; the frequency of interface demarcation was decreased by a factor of two after a short period of regrowth).

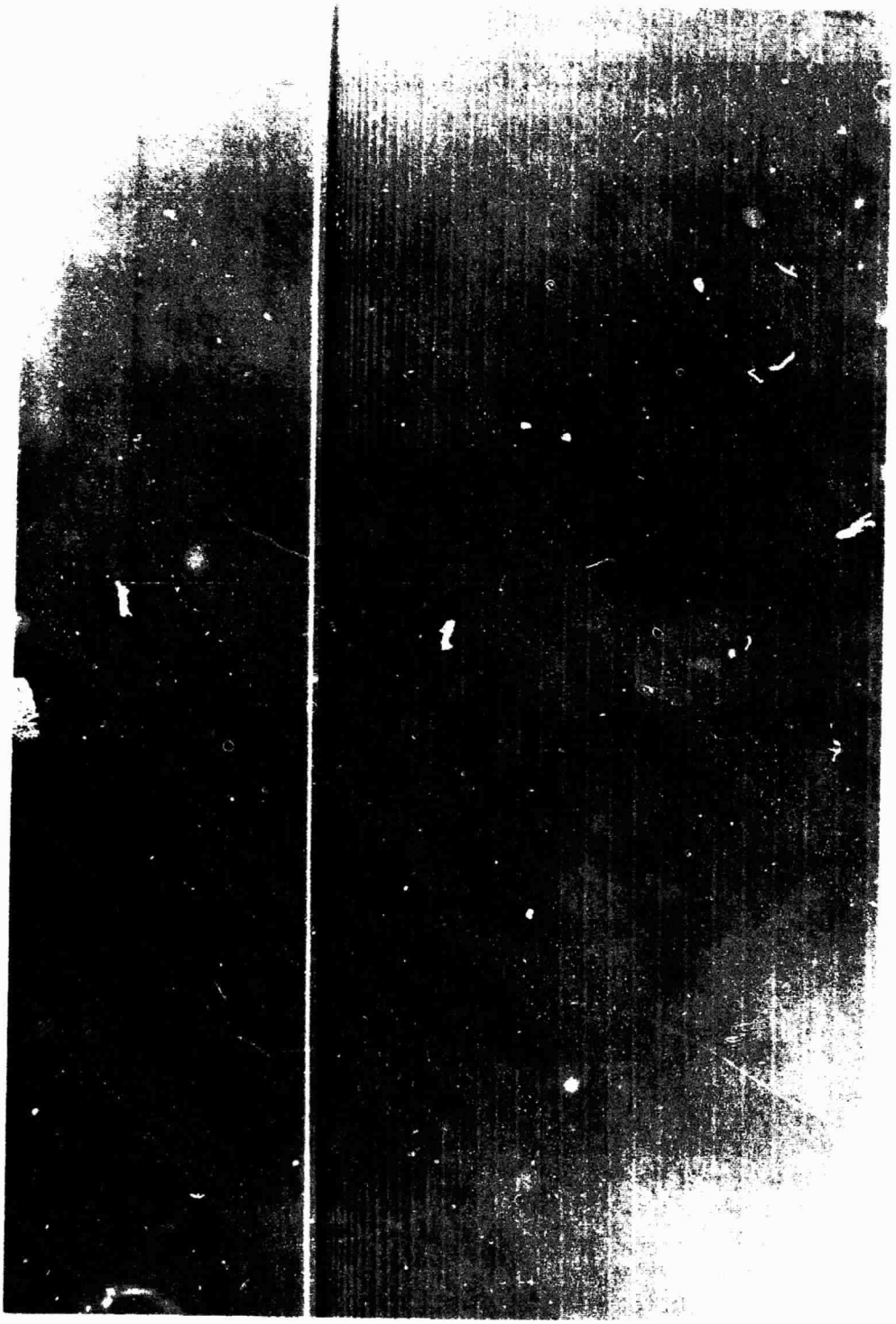

Figure V-23. Etched segment of <111> germanium crystal regrown during ground-based tests (the region depicted shows, through interface demarcation, the microscopic growth behavior associated with a thermal arrest of 1 h).

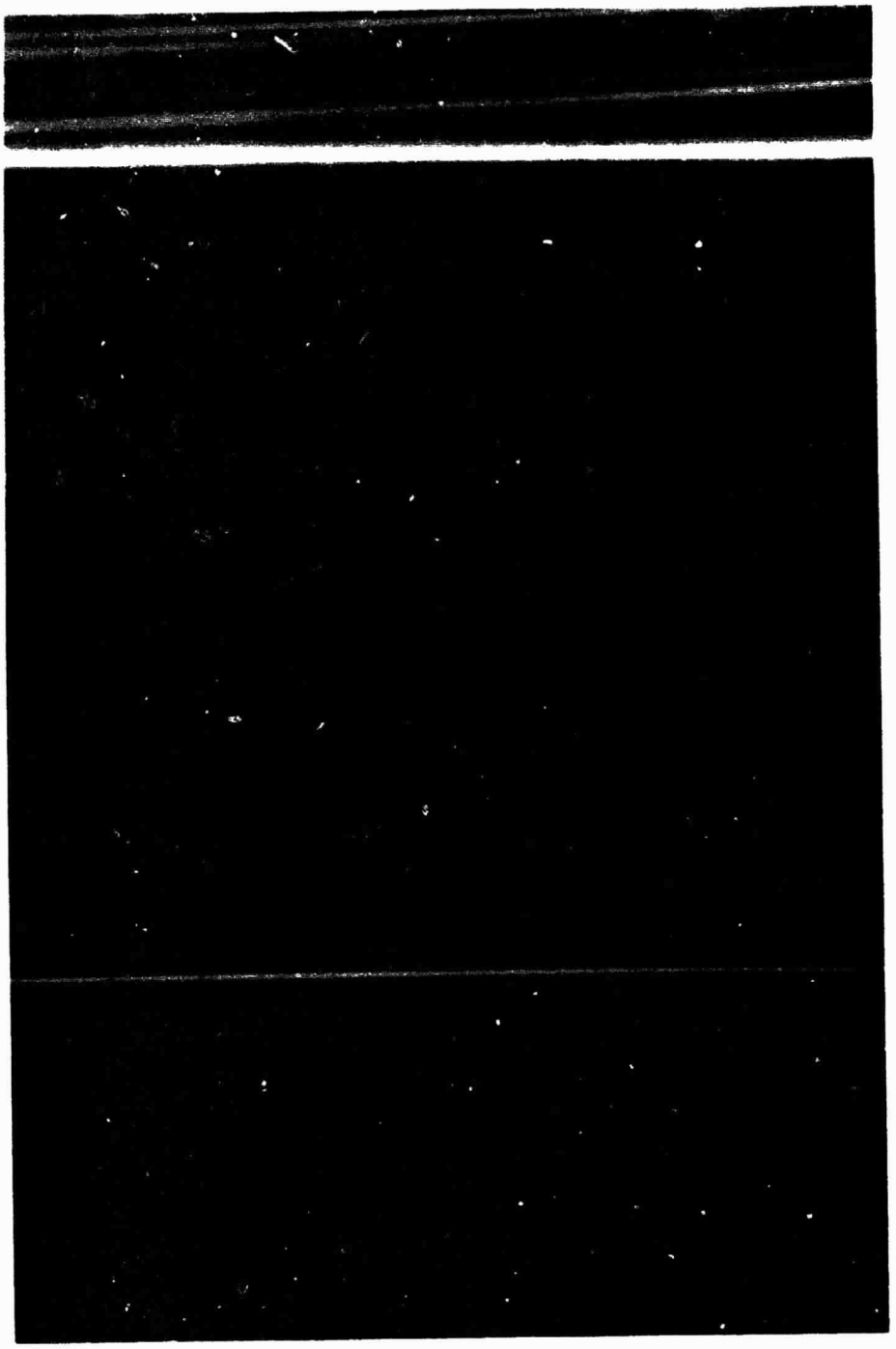

Figure V-24. Etched segment of a <100> germanium crystal regrown during ground-based tests at MSFC (notice the broad band of uncontrolled growth and segregation, 1000 μm, covering virtually all of the depicted region; this experiment was performed in the multipurpose furnace operated with line voltage) (110X)

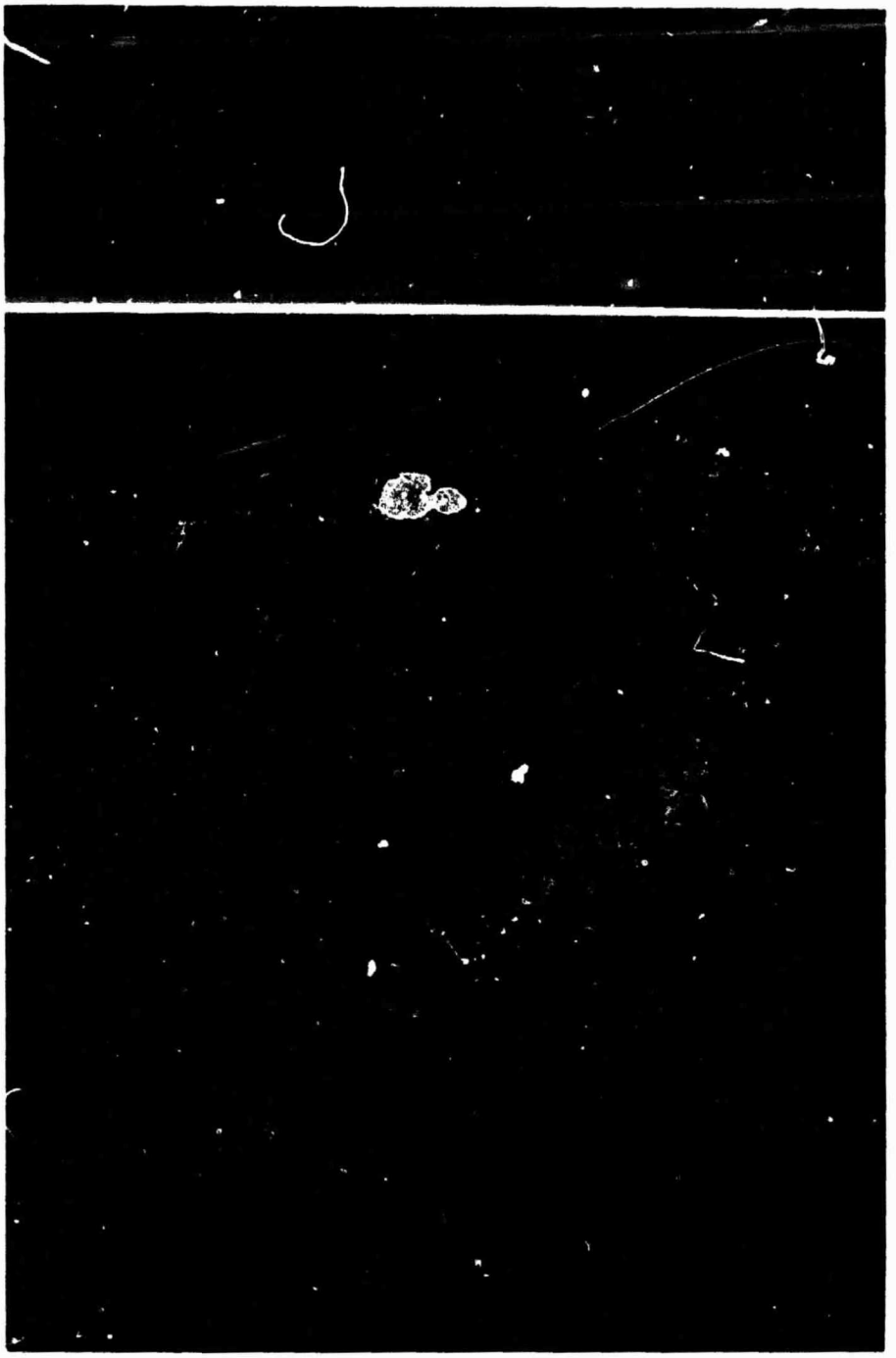

Figure V-25. Etched segment of a <100> germanium crystal regrown during ground-based tests at MSFC in the multipurpose furnace operated with battery power (notice that the band of uncontrolled growth and segregation immediately below the original regrowth interface has a width of 140 μm; compare with Figure V-24) (135X).

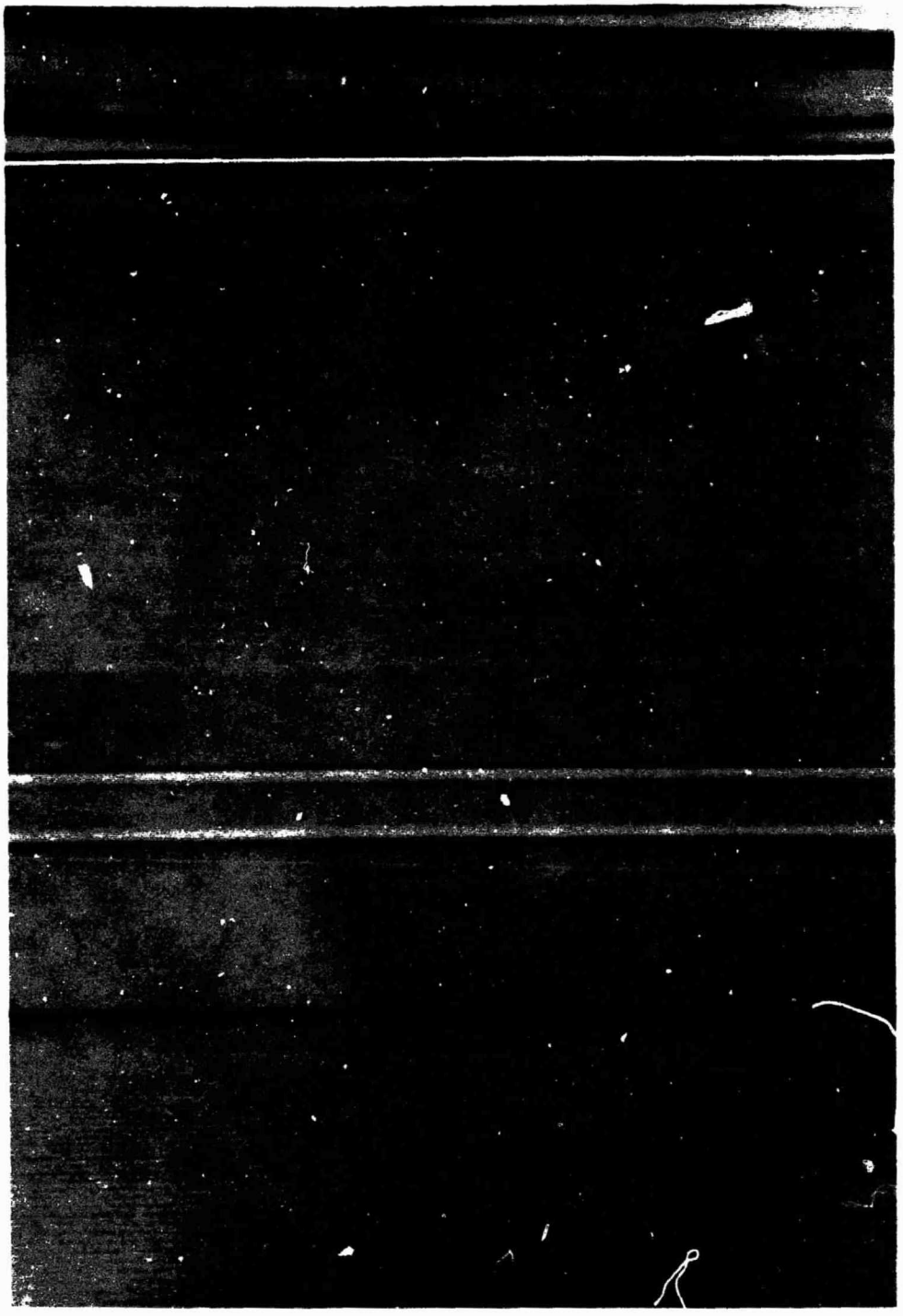

Figure V-26. Etched segment of a <111> germanium crystal regrown during the final ground-based test (GBT 3) (compare with Figure V-27) (210X).

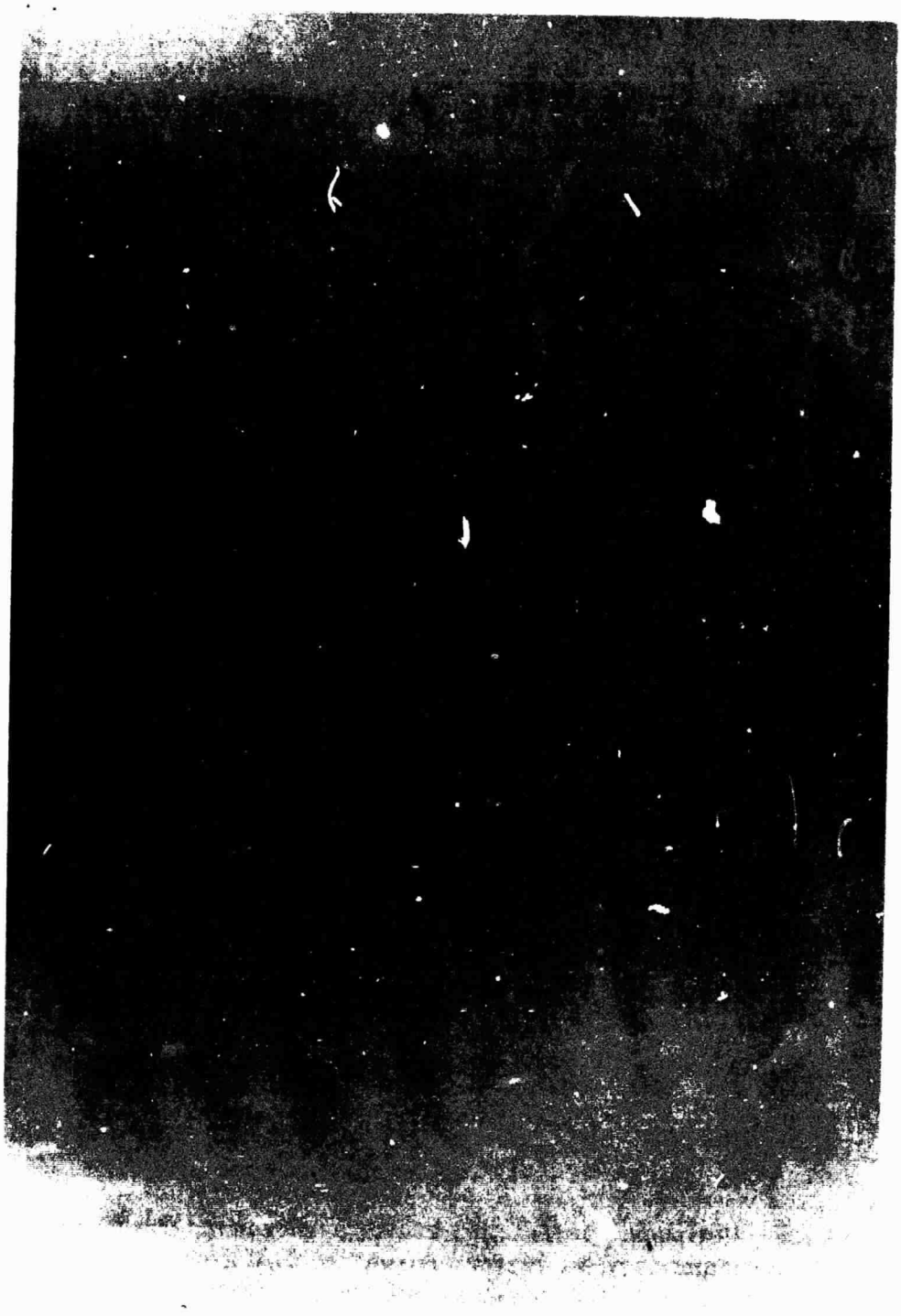

Figure V-27. Segregation inhomogeneities in <111> germanium crystal regrown during the final ground-based test (GBT 3) (the irregular dopant distribution appears after regrowth of approximately 1.0 cm; its origin is as yet unexplained).

Figure V-28. Peripheral segregation inhomogeneity in the cup region of the <111> germanium crystal regrown during the final ground-based test (GBT 3) (observe the appearance of a grain boundary; compare with Figure V-30).

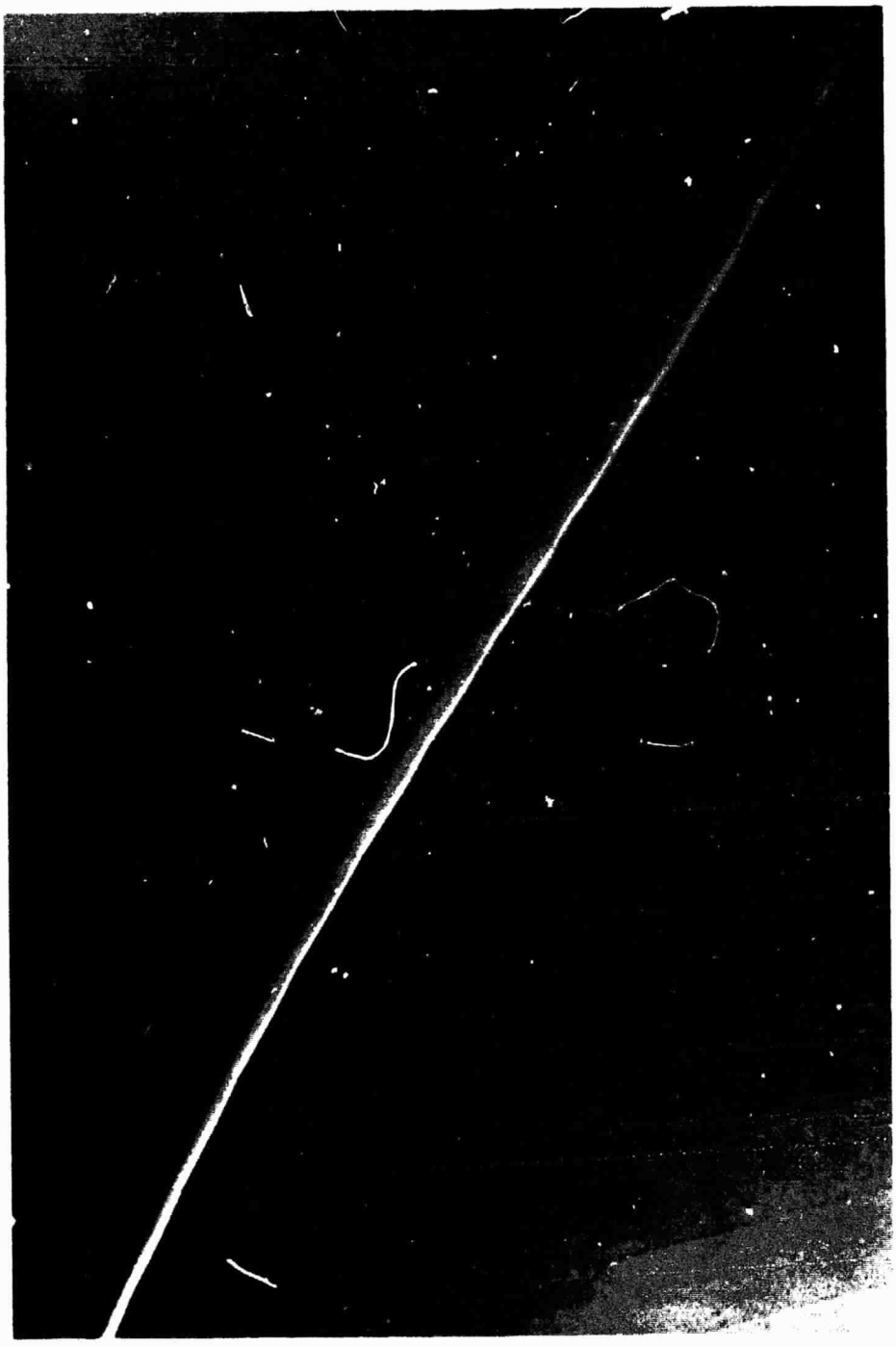

Figure V-29. Interface instability appearing in the central portion of the <111> germanium crystal regrown during the final ground-based test (GBT 3) (observe the development of severe growth interface distortion).

Figure V-30. Further development of interface instability and breakdown shown in Figure V-29.

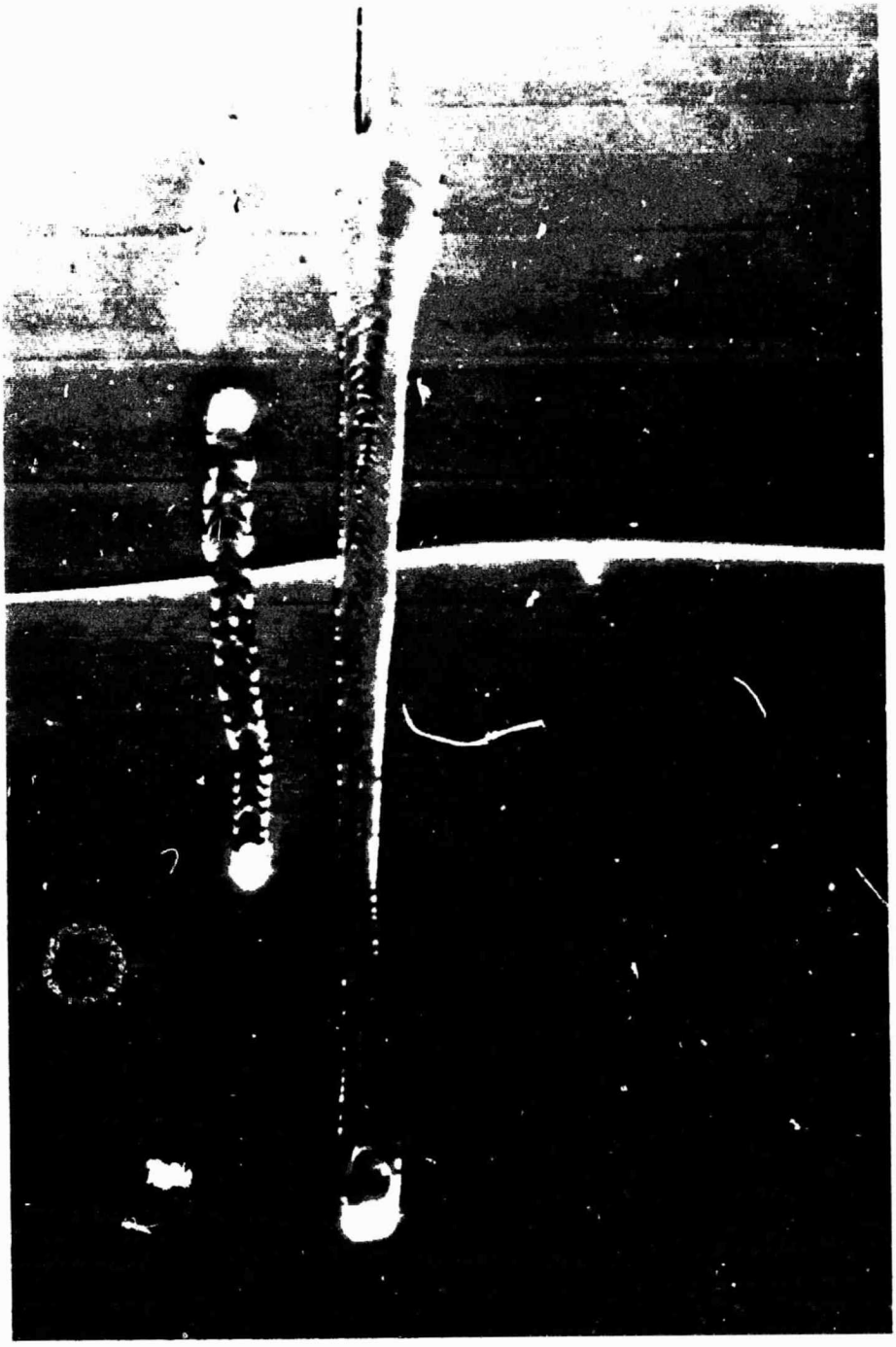

Figure V-31. Pronounced segregation inhomogeneity and phase segregation associated with the last stages of breakdown as depicted in Figures V-29 and V-30.

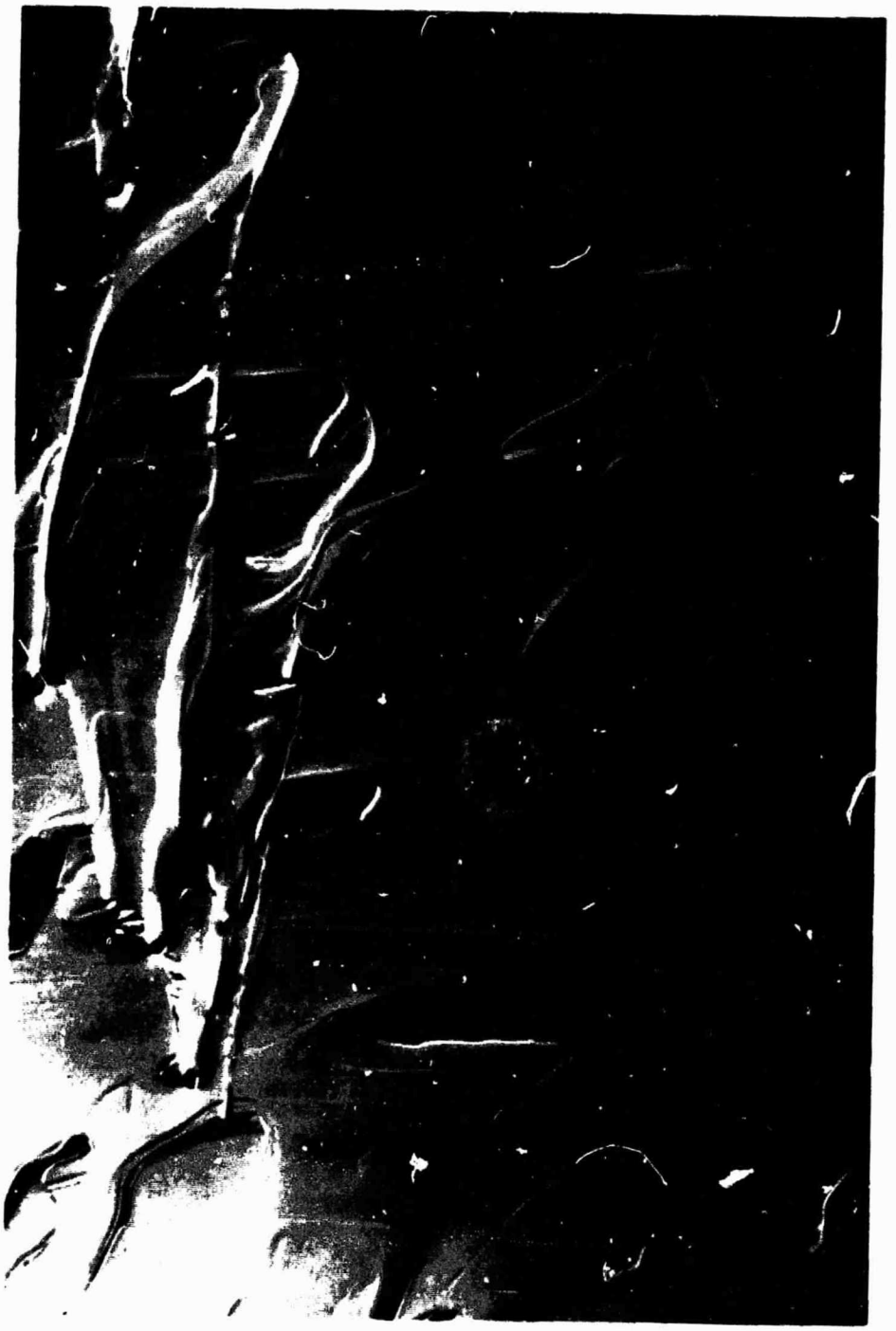

Figure V-32. Advanced stages of interface breakdown observed in the <111> germanium crystal regrown during the final ground-based test (GBT 3).

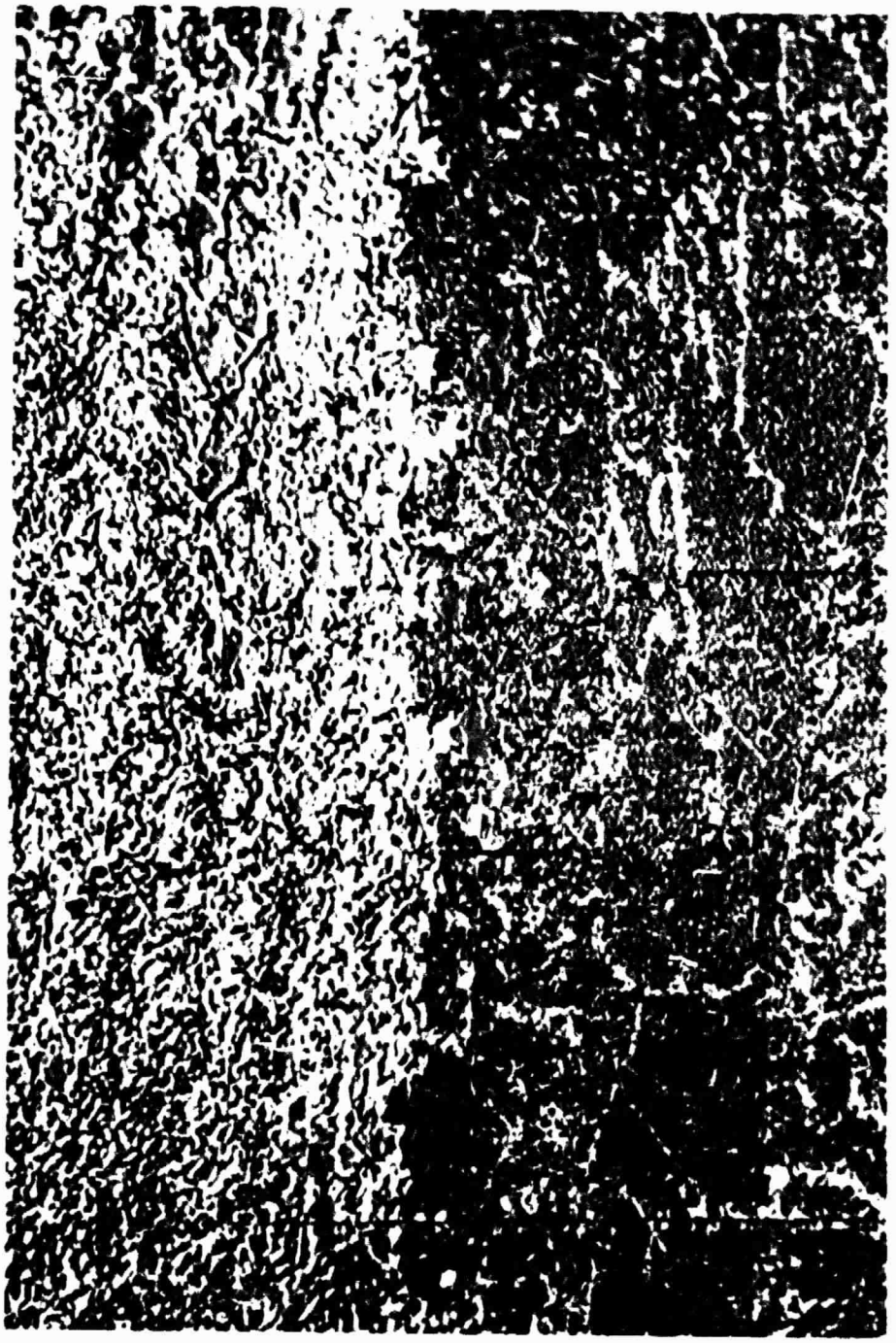

Figure V-33. Abrupt change in surface morphology observed in the <100> germanium crystal regrown during the final ground-based test (GBT 3).

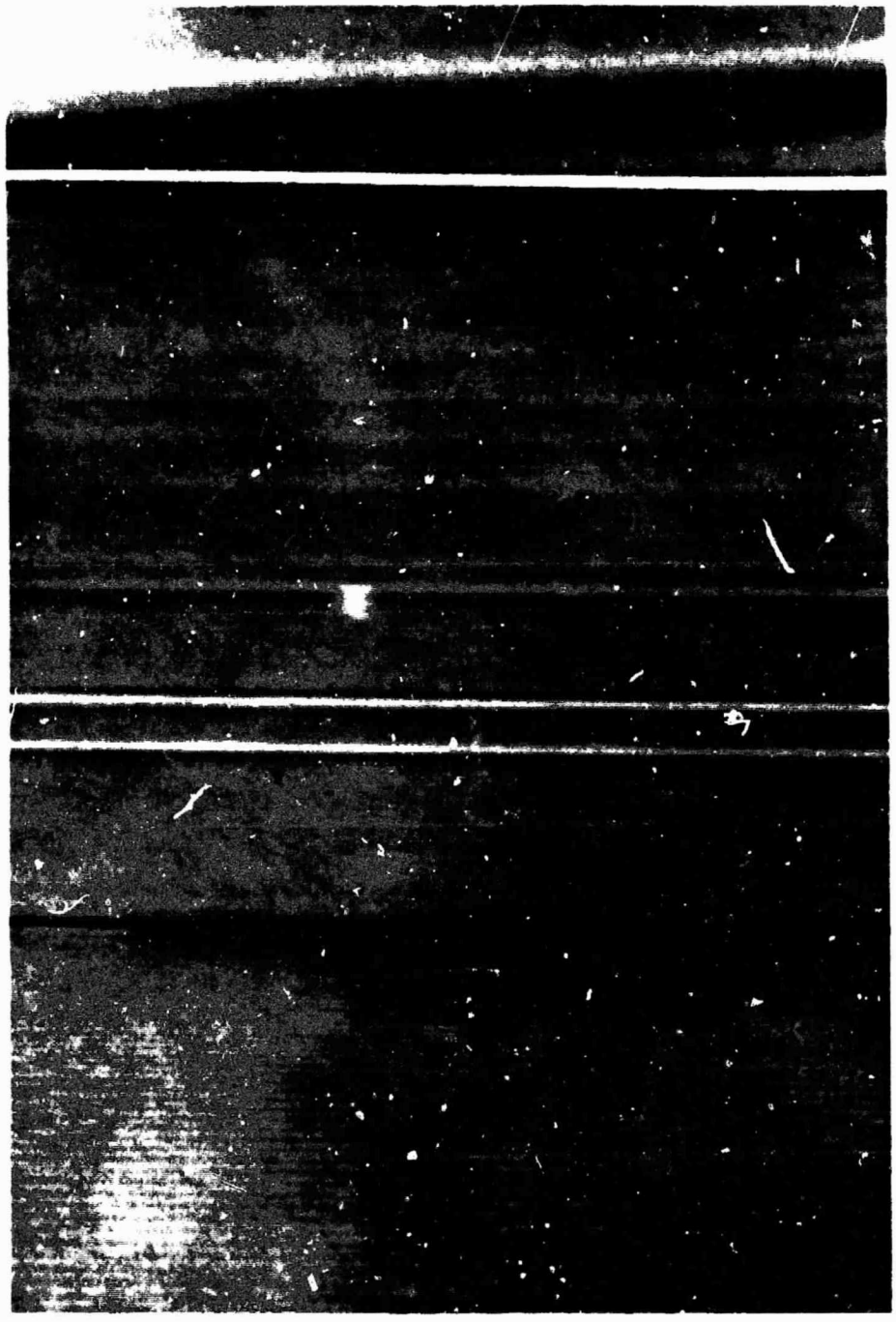

Figure V-34. Etched segment of <100> germanium crystal regrown during the final ground-based test (280X).

Figure V-35. Segregation inhomogeneities and interface breakdown in the <100> germanium crystal regrown during the final ground-based test (GBT 3).

Figure V-36. Advanced stage of interface breakdown in the <100> germanium crystal regrown during the final ground-based test (GBT 3).

EXPERIMENT	CRYSTAL	DOPANT	ORIENTATION	I/F BAND WIDTH μM	REGROWN LENGTH CM	SEED POLARITY	PULSE WIDTH MSEC	PULSE REP. RATE SEC	SOAK TIME HRS	COOLING RATE °C/MIN	I/F DEMARCATION VISIBILITY
SIM 1	S-1	GA	111	200	2.3	NEG	30	2	2	PASSIVE	FAINT
SIM 2	S-2	SN	111	NONE VISIBLE	2.1	NEG	60	4	2	.6	NOT DETECTED
PROTOTYPE	P-1	GA	100	0	3.8	NEG	60	4	2	.6	FAINT
	P-2	SB	100		4.0	NEG	60	4	2	.6	NOT DETECTED
	P-3	SN	100		3.9	NEG	60	4	2	.6	NOT DETECTED
GBT 1	A-5	GA	100	998	4.1	NEG	60	4	5	1.2, 40 MIN 2.4, 20 MIN 1.2, END	GOOD
	B-6	RE-RUN IN GBT 3									
	C-1	RE-RUN IN GBT 2									
GBT 2	A-1	GA	100	140	3.7	POS, 30 MIN NEG, END	60	4	2		GOOD
	B-1	SB	100	OVER TEMP. TEST, USED AS FILLER						2.4, 30 MIN THERMAL ARREST 2.4, END	
	C-1	GA	111	2150	3.7	POS, 30 MIN NEG, END	60	4	2		GOOD
GBT 3	A-6	GA	100	336	4.1	POS	55	3.95	2	2.4	GOOD
	B-6	SB	100		3.6	POS	55	3.95	2	2.4	NOT DETECTED
	C-6	GA	111	511	4.0	POS	55	3.95	2	2.4	GOOD

Figure V-37. Tabulation of MA-060 ground-based tests.

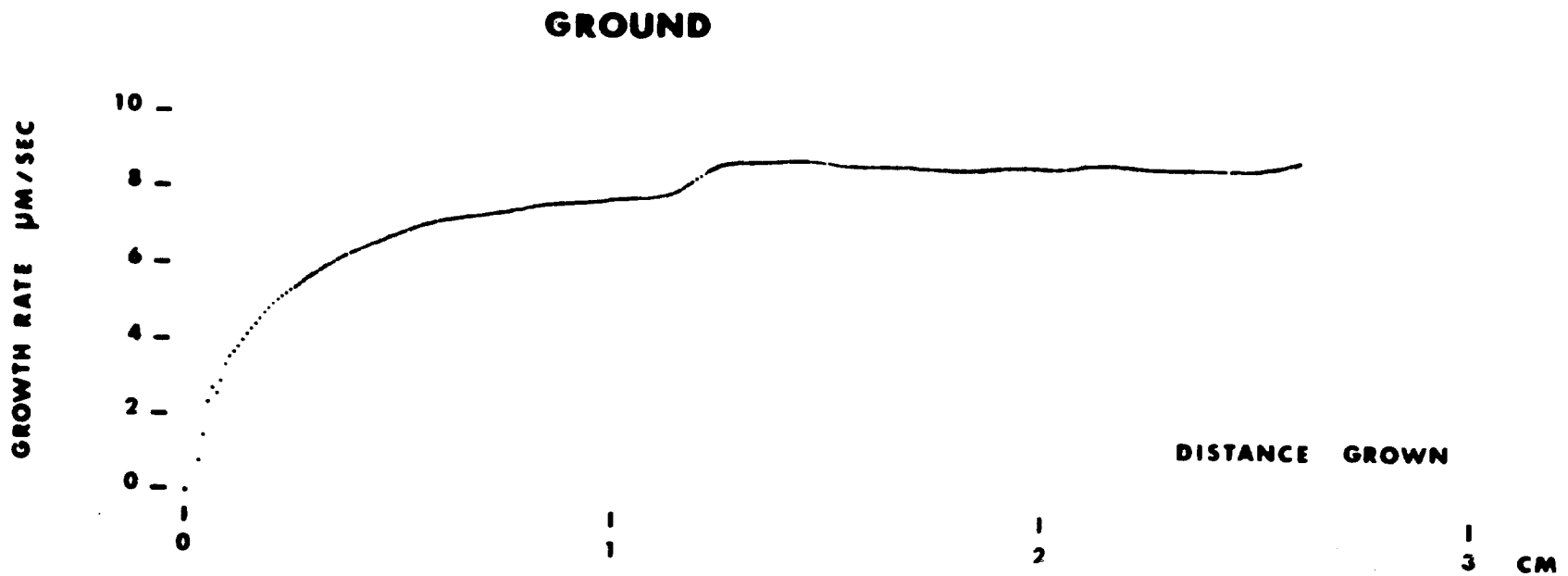

Figure V-38. Microscopic growth rates of the <111> germanium crystal regrown during the final ground-based test (GBT 3).

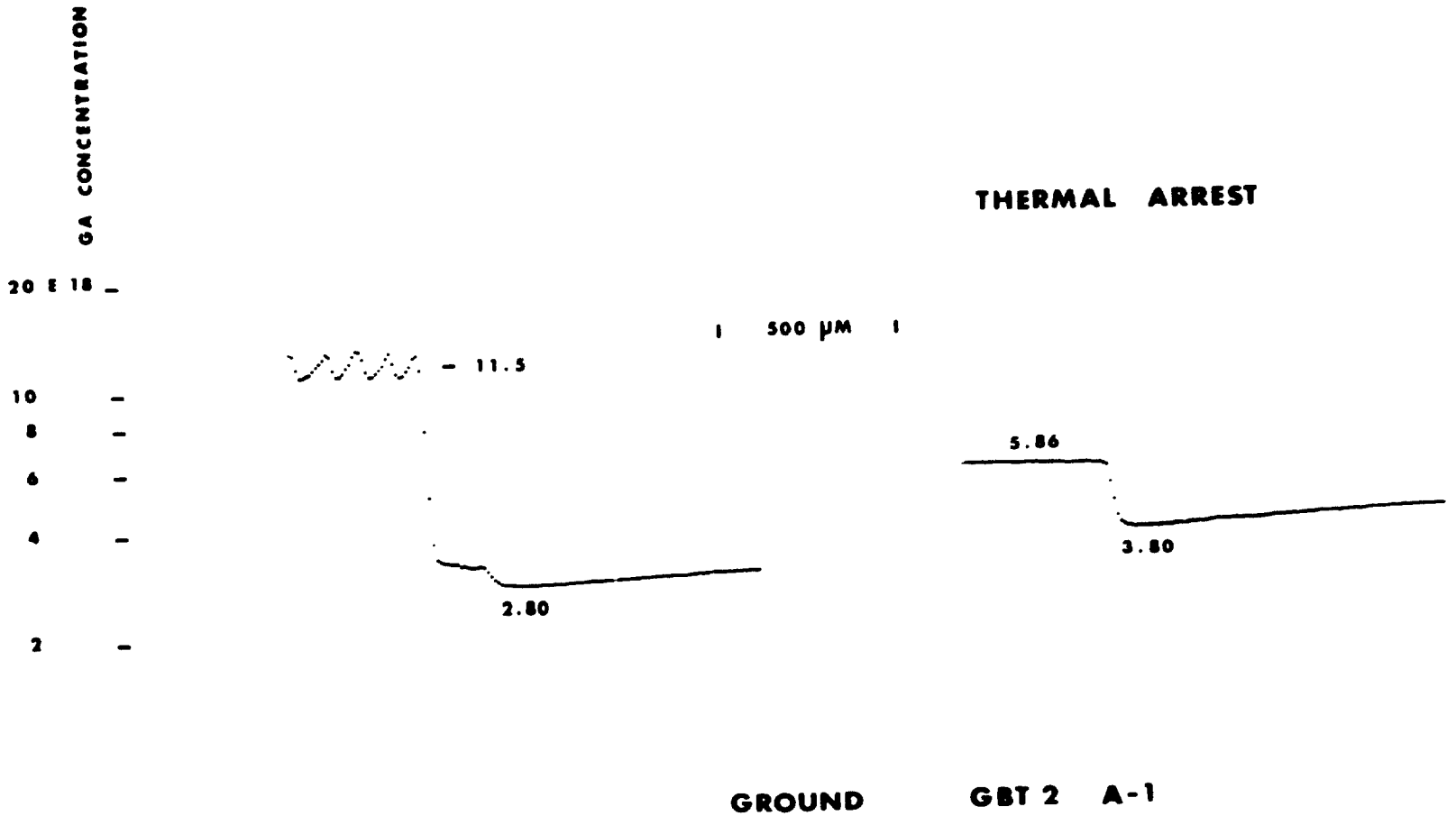

Figure V-39. Compositional profiles of the initial regrowth region and a thermal arrest in a <100> germanium crystal regrown during the second ground-based test (GBT 2).

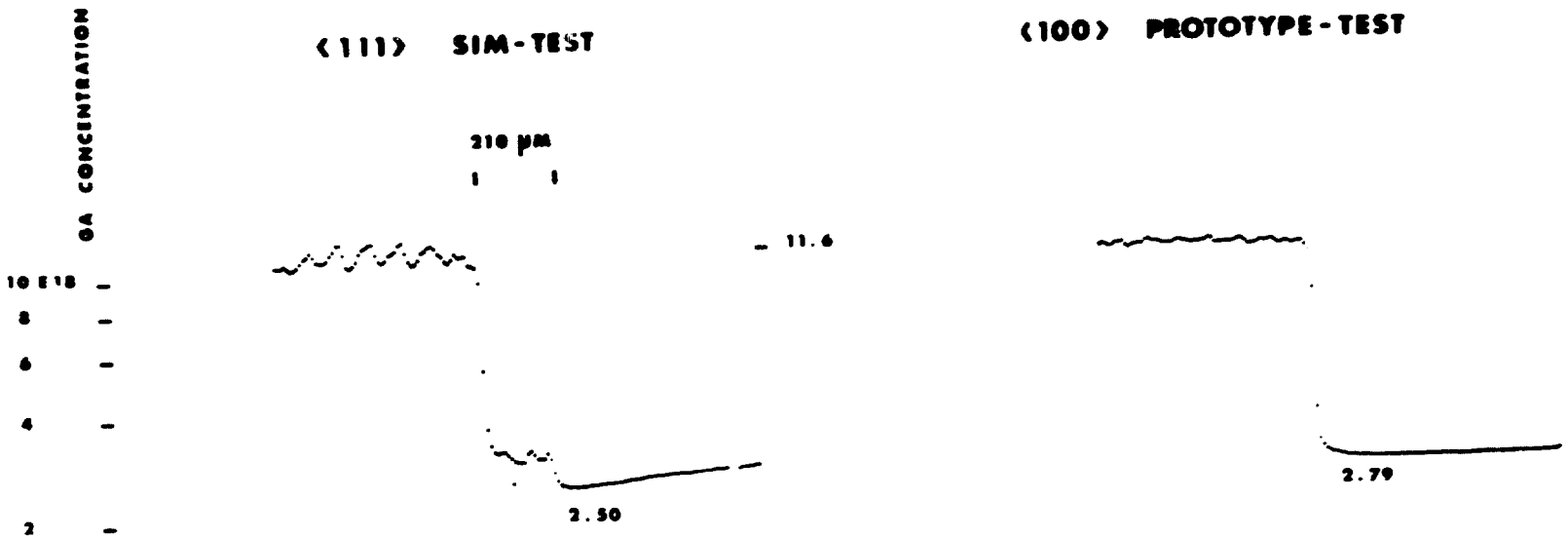

Figure V-40. Compositional profiles of the initial regrowth regions of germanium crystals regrown during simulation and prototype tests.

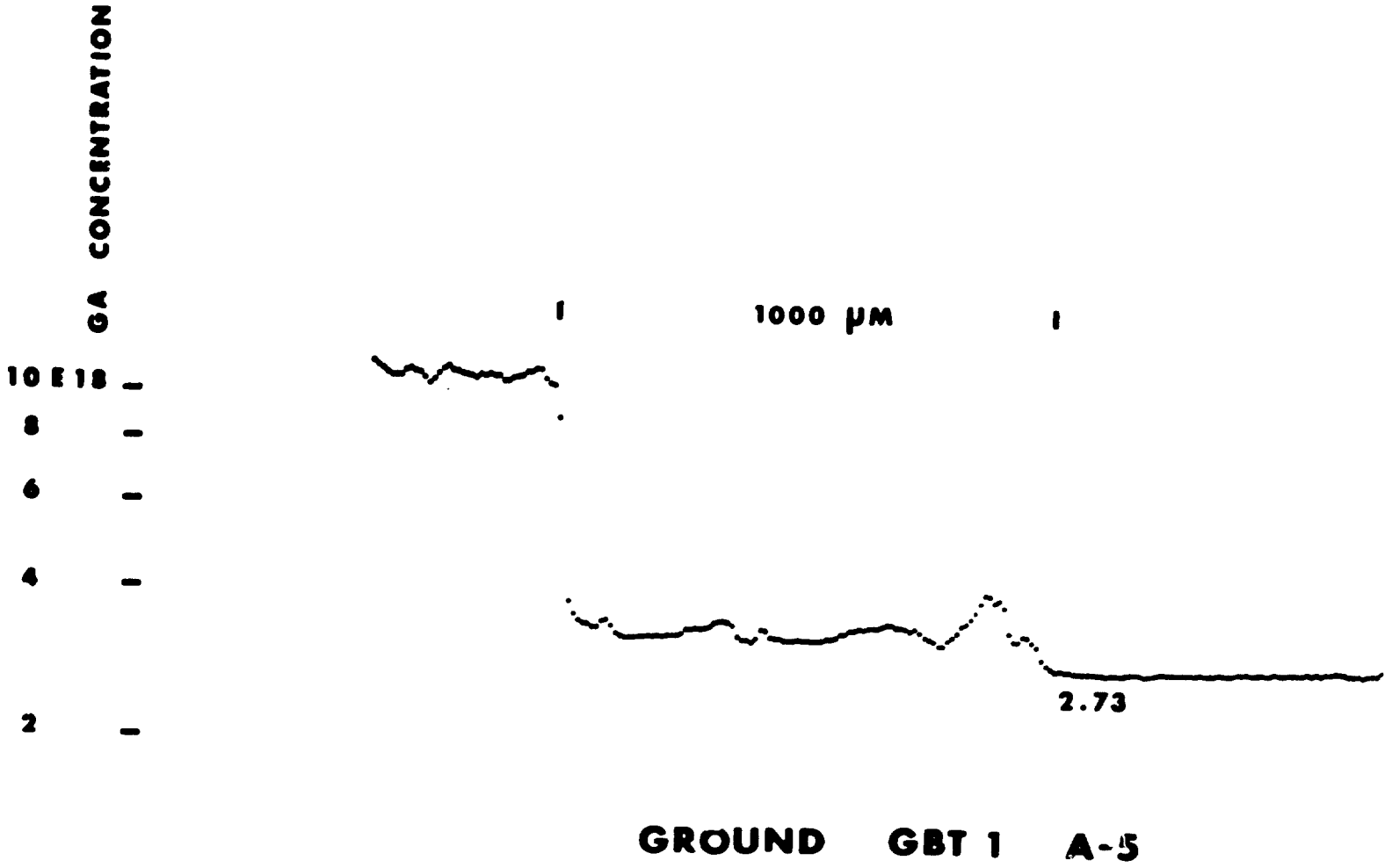

Figure V-41. Compositional profile of initial regrowth region in a <100> germanium crystal regrown during the first ground-based test (GBT 1) (notice the pronounced compositional fluctuations associated with uncontrolled growth, 1000 μm).

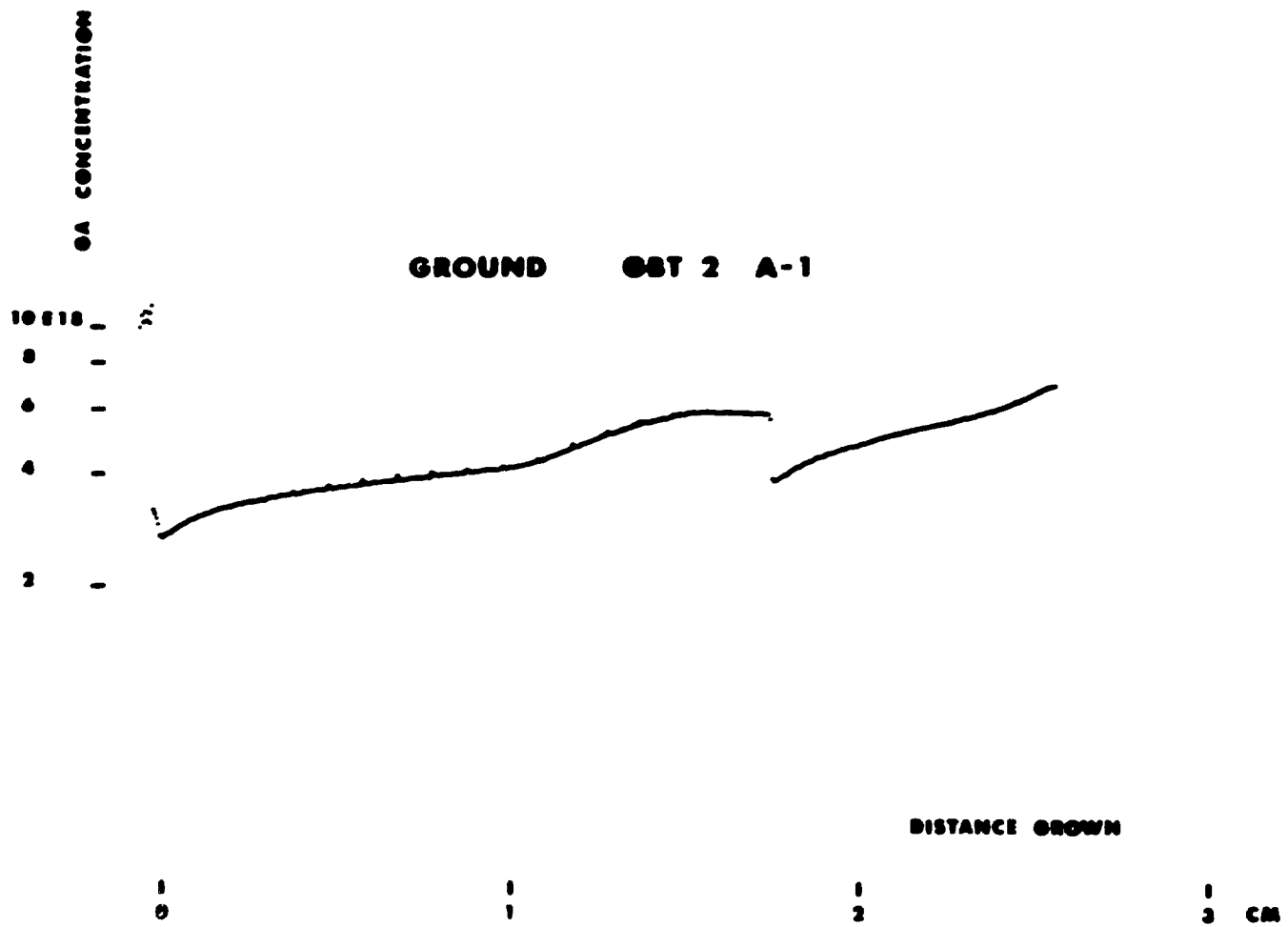

Figure V-42. Compositional profile in a <100> germanium crystal regrown with a thermal arrest of 1 h.

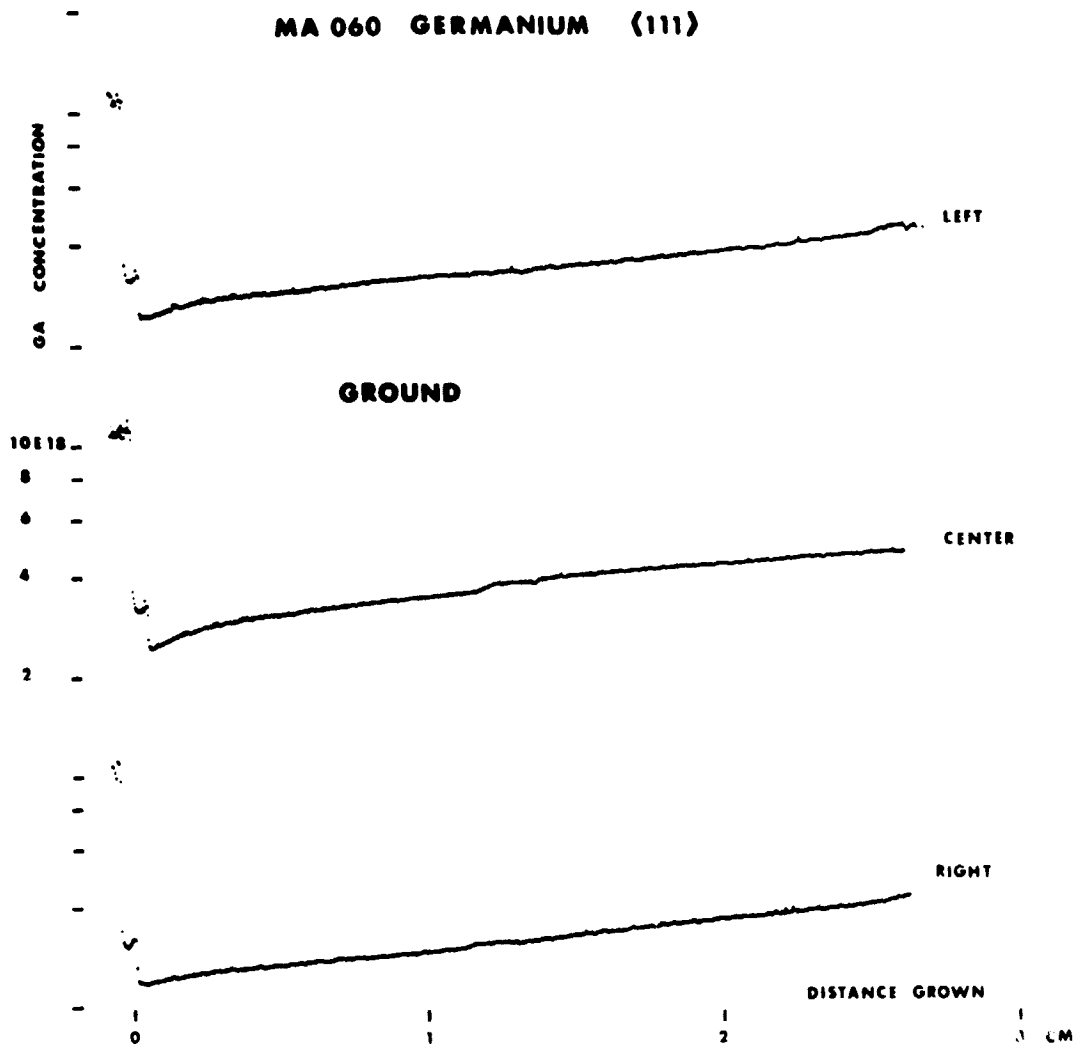

Figure V-43. Macroscopic compositional profiles of the <111> germanium crystal regrown during ground-based test (GBT 3).

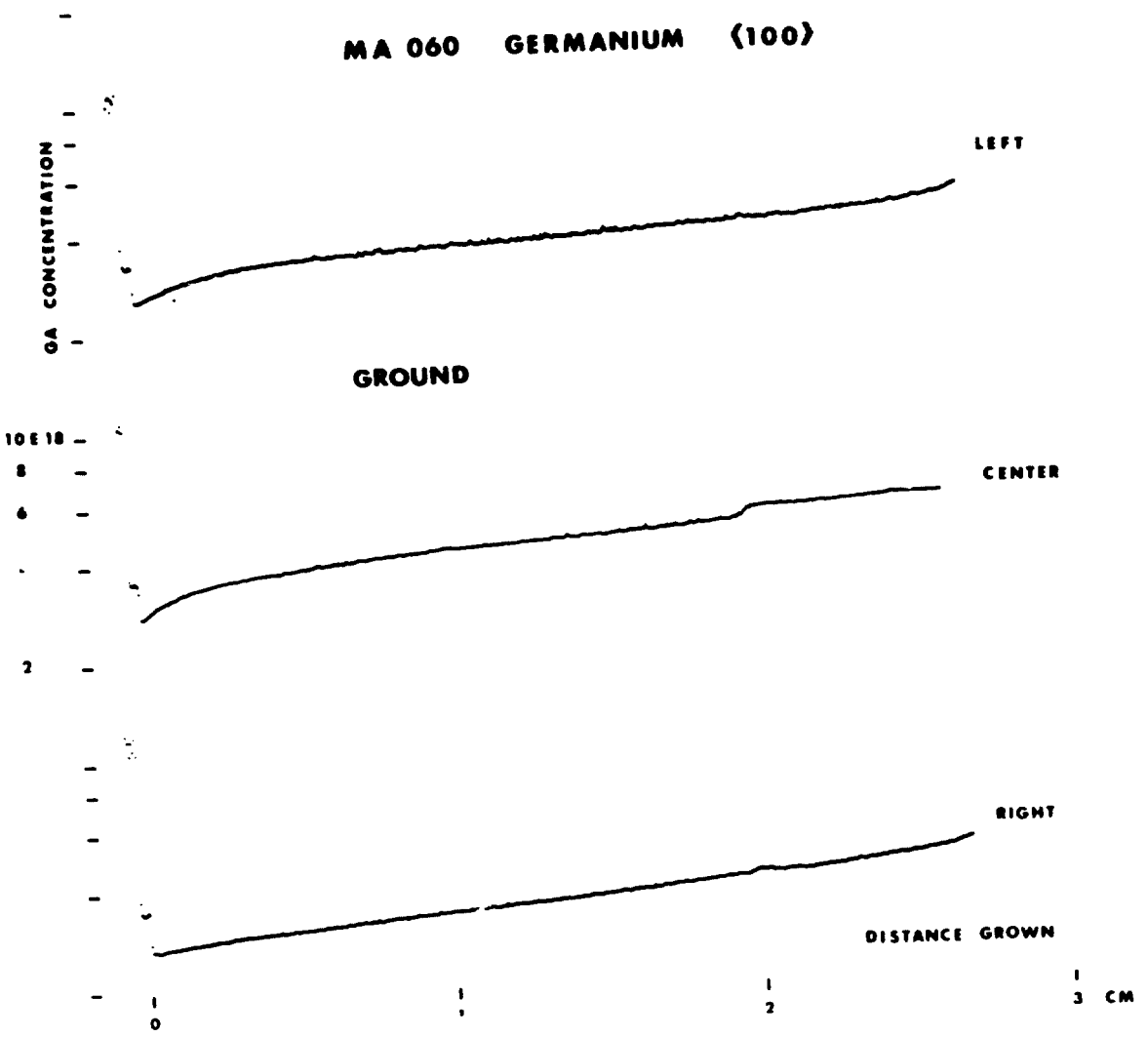

Figure V-44. Macroscopic compositional profiles of the <100> germanium crystal regrown during ground-based test (GBT 3).

ACKNOWLEDGMENTS

The authors are grateful to the National Aeronautics and Space Administration, particularly to the staff at Marshall Space Flight Center for their cooperation and enthusiastic support during all stages of the experiment. They are indebted to Mr. J. Baker for his skillful assistance with the characterization program and to Ms. M. Cretella and Messrs. D. Holmes and E. Martin for their valuable contributions to this work.

REFERENCES

V-1. Skylab Science Experiments. Vol. 38, Science and Technology, American Astronautical Society, 1975.

V-2. Witt, A. F.; Lichtensteiger, J.; and Gatos, H. C.: Experimental Approach to the Quantitative Determination of Dopant Segregation During Crystal Growth on a Microscale: Ga Doped Ge. J. Electrochem. Soc., vol. 120, 1973, pg. 1119.

V-3. Mazur, R. G. and Dickey, D. H.: J. Electrochem. Soc., vol. 113, 1966, p. 255.

V-4. Sze, S. M. and Irvin, J. C.: Solid State Electronics, vol. 11, 1968, p. 599.

V-5. Witt, A. F.; Lichtensteiger, M.; and Gatos, H. C.: J. Electrochem. Soc., vol. 120, 1973, p. 1119.

V-6. Van der Pauw, L. J.: Philips Res. Rep., vol. 13, 1958, p. 1.

BIBLIOGRAPHY

Brice, J. C.: The Growth of Crystals from Liquids. North-Holland Publishing Co., 1973.

Chalmers, B.: The Principles of Solidification. J. Wiley, 1964.

Gilman, J. J., Ed.: The Art and Science of Growing Crystals. J. Wiley, 1963.

Witt, A. F.; Gatos, H. C.; Lichtensteiger, M.; Cretella, M.; and Herman, C. J.: Crystal Growth and Steady-State Segregation under Zero Gravity: InSb. J. Electrochem. Soc., vol. 122, 1975, p. 276.